

1 **Sensitivity of a leaf gas-exchange model for estimating paleoatmospheric CO<sub>2</sub>  
2 concentration**

4 **Dana L. Royer<sup>1</sup>, Kylen M. Moynihan<sup>1</sup>, Melissa L. McKee<sup>1</sup>, Liliana Londoño<sup>2</sup>, and Peter J. Franks<sup>3</sup>**

5 <sup>1</sup>Department of Earth and Environmental Sciences, Wesleyan University, Middletown, Connecticut, USA

6 <sup>2</sup>Smithsonian Tropical Research Institute, Balboa, Ancón, Republic of Panamá

7 <sup>3</sup>Faculty of Agriculture and Environment, University of Sydney, Sydney, New South Wales, Australia

8 **Correspondence:** Dana L. Royer (droyer@wesleyan.edu)

10  
11 **Abstract.** Leaf gas-exchange models show considerable promise as paleo-CO<sub>2</sub> proxies. They are largely  
12 mechanistic in nature, provide well-constrained estimates even when CO<sub>2</sub> is high, and can be applied to  
13 most subaerial, stomata-bearing fossil leaves from C<sub>3</sub> taxa, regardless of age or taxonomy. Here we  
14 place additional observational and theoretical constraints on one of these models, the “Franks” model.  
15 In order to gauge the model’s general accuracy in a way that is appropriate for fossil studies, we  
16 estimated CO<sub>2</sub> from 40 species of extant angiosperms, conifers, and ferns based only on measurements  
17 that can be made directly from fossils (leaf δ<sup>13</sup>C and stomatal density and size) and on a limited sample  
18 size (1-3 leaves per species). The mean error rate is 28%, which is similar to or better than the accuracy  
19 of other leading paleo-CO<sub>2</sub> proxies. We find that leaf temperature and photorespiration do not strongly  
20 affect estimated CO<sub>2</sub>, although more work is warranted on the possible influence of O<sub>2</sub> concentration on  
21 photorespiration. Leaves from the lowermost 1-2 m of closed-canopy forests should not be used  
22 because the local air δ<sup>13</sup>C value is lower than the global well-mixed value. Such leaves are not common  
23 in the fossil record, but can be identified by morphological and isotopic means.

24  
25 **1 Introduction**

26 Leaves on terrestrial plants are well poised to record information about the concentration of  
27 atmospheric CO<sub>2</sub>. They are in direct contact with the atmosphere and have large surface-area-to-volume  
28 ratios, so the leaf internal CO<sub>2</sub> concentration is tightly coupled to atmospheric CO<sub>2</sub> concentration. Also,  
29 leaves are specifically built for the purpose of fixing atmospheric carbon into structural tissue, and face  
30 constant selection pressure to optimize their carbon uptake relative to water loss. As a result, many  
31 components of the leaf system are sensitive to atmospheric CO<sub>2</sub>, and these components feedback on  
32 one another to reach a new equilibrium when atmospheric CO<sub>2</sub> changes. In terms of carbon assimilation,  
33 Farquhar and Sharkey (1982) modeled this system in its simplest form as:

34  
35 
$$A_n = g_{c(tot)} \times (c_a - c_i), \quad (1)$$

36 where  $A_n$  is the leaf CO<sub>2</sub> assimilation rate (μmol m<sup>-2</sup> s<sup>-1</sup>),  $g_{c(tot)}$  is the total operational conductance to CO<sub>2</sub>  
37 diffusion from the atmosphere to site of photosynthesis (mol m<sup>-2</sup> s<sup>-1</sup>),  $c_a$  is atmospheric CO<sub>2</sub>  
38 concentration (μmol mol<sup>-1</sup> or ppm), and  $c_i$  is leaf intercellular CO<sub>2</sub> concentration (μmol mol<sup>-1</sup> or ppm)  
39 (see also Von Caemmerer, 2000).

40 Rearranging Eq. (1) for atmospheric CO<sub>2</sub> yields:

41  
42 
$$c_a = \frac{A_n}{g_{c(tot)} \times (1 - \frac{c_i}{c_a})}. \quad (2)$$

47 Equation (2) forms the basis of two leaf gas-exchange approaches for estimating paleo-CO<sub>2</sub> from fossils  
 48 (Konrad et al., 2008, 2017; Franks et al., 2014). In the Franks model, conductance is estimated in part  
 49 from measurements of stomatal size and density,  $c_i/c_a$  from measurements of leaf  $\delta^{13}\text{C}$  along with  
 50 reconstructions of coeval air  $\delta^{13}\text{C}$  (see also Eq. 9), and  $A_n$  from knowledge of living relatives and its  
 51 dependency on  $c_a$  (Franks et al., 2014). Following Farquhar et al. (1980), the latter is modeled as (Franks  
 52 et al., 2014; Kowalczyk et al., 2018):  
 53

$$54 A_n = A_0 \frac{\left[\left(\frac{c_i}{c_a}\right)c_a - \Gamma^*\right]\left[\left(\frac{c_{i0}}{c_{ao}}\right)c_{ao} + 2\Gamma^*\right]}{\left[\left(\frac{c_i}{c_a}\right)c_a + 2\Gamma^*\right]\left[\left(\frac{c_{i0}}{c_{ao}}\right)c_{ao} - \Gamma^*\right]}, \quad (3)$$

55 where  $\Gamma^*$  is the CO<sub>2</sub> compensation point in the absence of dark respiration (ppm) and the subscript "0"  
 56 refers to conditions at a known CO<sub>2</sub> concentration (typically present-day). Equations (2) and (3) are then  
 57 solved iteratively until the solution for  $c_a$  converges.  
 58

59 These gas-exchange approaches grew out of a group of paleo-CO<sub>2</sub> proxies based on the CO<sub>2</sub>  
 60 sensitivity of stomatal density ( $D$ ) or the similar metric stomatal index (Woodward, 1987; Royer, 2001).  
 61 Here, the  $D$ - $c_a$  sensitivity is calibrated in an extant species, allowing paleo-CO<sub>2</sub> inference from the same  
 62 (or very similar) fossil species. These empirical relationships typically follow a power-law function  
 63 (Wynn, 2003; Franks et al., 2014; Konrad et al., 2017):  
 64

$$65 c_a = \frac{1}{kD^\alpha}, \quad (4)$$

66 where  $k$  and  $\alpha$  are species-specific constants.  
 67

68 The related stomatal ratio proxy is simplified:  $D$  is measured in an extant species ( $D_0$ , at present-  
 69 day  $c_{ao}$ ) and then the ratio of  $D_0$  to  $D$  in a related fossil species is assumed to be linearly related to the  
 70 ratio of paleo- $c_a$  to present-day  $c_{ao}$  (Chaloner and McElwain, 1997; McElwain, 1998):  
 71

$$72 \frac{c_a}{c_{ao}} = k \frac{D_0}{D}. \quad (5)$$

73 Equation (5) can be rearranged to match Eq. (4) but with  $\alpha$  fixed at 1. Thus, paleo-CO<sub>2</sub> estimates using  
 74 the stomatal ratio proxy are based on a one-point calibration and an assumption that  $\alpha = 1$ ;  
 75 observations do not always support this assumption (e.g.,  $\alpha = 0.43$  for *Ginkgo biloba*; Barclay and Wing,  
 76 2016). The scalar  $k$  was originally set at 2 for Paleozoic and Mesozoic reconstructions so that paleo-CO<sub>2</sub>  
 77 estimates during the Carboniferous matched that from long-term carbon cycle models (Chaloner and  
 78 McElwain, 1997). For younger reconstructions,  $k$  is probably closer to 1 (by definition,  $k = 1$  for present-  
 79 day plants). We note that the stomatal ratio proxy was originally conceived as providing qualitative  
 80 information, only, about paleo-CO<sub>2</sub> (McElwain and Chaloner, 1995, 1996; Chaloner and McElwain, 1997;  
 81 McElwain, 1998) and has not been tested with dated herbaria materials or with CO<sub>2</sub> manipulation  
 82 experiments.  
 83

84 At high CO<sub>2</sub>, the  $D$ - $c_a$  sensitivity saturates in many species, leading to uncertain paleo-CO<sub>2</sub>  
 85 estimates, often with unbounded upper limits (e.g., Smith et al., 2010; Doria et al., 2011). Stomatal  
 86 density does not respond to CO<sub>2</sub> in all species (Woodward and Kelly, 1995; Royer, 2001), and because  $D$ -  
 87  $c_a$  relationships can be species-specific (that is, different species in the same genus with different  
 88 responses; Beerling, 2005; Haworth et al., 2010), only fossil taxa that are still alive today should be used.  
 89 The gas-exchange proxies partly address these limitations: 1) CO<sub>2</sub> estimates remain well-bounded—even  
 90 at high CO<sub>2</sub>—and their precision is similar to or better than other leading paleo-CO<sub>2</sub> proxies (~+35/-25%  
 91 at 95% confidence; Franks et al., 2014); 2) the models are mostly mechanistic; that is, they are explicitly

92 driven by plant physiological principles, not just empirical relationships measured on living plants; 3)  
93 because the models retain sensitivity at high CO<sub>2</sub> and do not require that a fossil species still be alive  
94 today, much of the paleobotanical record is open for CO<sub>2</sub> inference, regardless of age or taxonomy; and  
95 4) because the models are based on multiple inputs linked by feedbacks, they can still perform  
96 adequately even if one or more of the inputs in a particular taxon is not sensitive to CO<sub>2</sub>, for example  
97 stomatal density (Milligan et al., 2019).

98 We note that the published uncertainties (= precision) associated with the stomatal density  
99 proxies are probably too small because they usually only reflect uncertainty in either the calibration  
100 regression or in the measured values of fossil stomatal density, but not both; when both sources are  
101 propagated, errors often exceed ±30% at 95% confidence (Beerling et al., 2009). Also, error rates in  
102 estimates from extant taxa where CO<sub>2</sub> is known (= accuracy) are usually smaller with stomatal density  
103 proxies than with gas-exchange proxies (e.g., Barclay and Wing, 2016), but this is expected because the  
104 same taxa have been calibrated in present-day (or near present-day) conditions. Because the gas-  
105 exchange proxies are largely built from physiological principles, they have less “recency” bias; that is, the  
106 gas-exchange proxies estimate present-day and paleo-CO<sub>2</sub> with similar certainty when the same  
107 methods are used to determine the inputs.

## 110 **2 Study Aims and Methods**

112 Leaf gas-exchange proxies for paleo-CO<sub>2</sub> are becoming popular (Konrad et al., 2008, 2017; Grein  
113 et al., 2011a, 2011b, 2013; Erdei et al., 2012; Roth-Nebelsick et al., 2012, 2014; Franks et al., 2014;  
114 Maxbauer et al., 2014; Montañez et al., 2016; Reichgelt et al., 2016; Tesfamichael et al., 2017; Kowalczyk  
115 et al., 2018; Lei et al., 2018; Londoño et al., 2018; Richey et al., 2018; Milligan et al., 2019). However,  
116 many elements in these models remain understudied. Here we scrutinize four such elements of the  
117 Franks et al. (2014) model, and ask: how does the model perform across a large number of  
118 phylogenetically diverse taxa; and how is the model affected by temperature, photorespiration, and  
119 proximity to the forest floor? We describe next the motivation and details of the study design (see also  
120 Table 1 for summary).

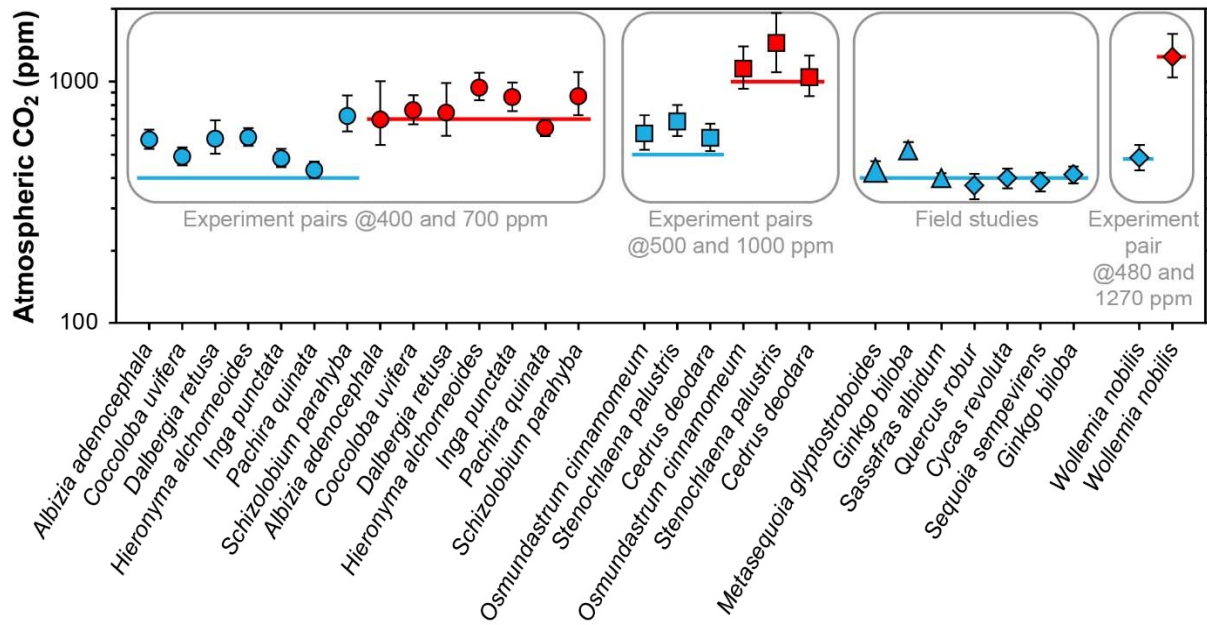
122 **Table 1.** Attributes of data sets used to test the Franks et al. (2014) model.

Element of model tested	Number of species	Methods section	Notes
General testing in a phylogenetically diverse set of species and with a minimal number of leaves measured per species	40	2.1	Leaves come from Panama (published by Londoño et al., 2018), Connecticut, and Puerto Rico
Temperature	6	2.2	Theoretical calculations and growth chamber experiment
Photorespiration	NA	2.3	Theoretical calculations
Canopy position	6	2.4	Leaves come from Panama and Connecticut

### 125 2.1 General testing in living plants

126  
127 Franks et al. (2014) tested the model on four species of field-grown trees (three gymnosperms and one  
128 angiosperm) and one conifer grown in chambers at 480 and 1270 ppm CO<sub>2</sub>. The average error rate  
129 (absolute value of estimated CO<sub>2</sub> minus measured CO<sub>2</sub>, divided by measured CO<sub>2</sub>) was 5%. Follow-up

130 work with three field-grown tree species (Maxbauer et al., 2014; Kowalczyk et al., 2018), CO<sub>2</sub>  
 131 experiments on seven tropical trees species (Londoño et al., 2018), and experiments on two fern and  
 132 one conifer species (Milligan et al., 2019) indicate somewhat higher error rates (Fig. 1). Combined, the  
 133 average error rate is 20% (median = 13%).



134  
 135 **Figure 1.** Published CO<sub>2</sub> estimates using the Franks model for extant plants where the physiological  
 136 inputs  $A_0$  (assimilation rate at a known CO<sub>2</sub> concentration) and/or  $g_{c(op)}/g_{c(max)}$  (ratio of operational to  
 137 maximum leaf conductance to CO<sub>2</sub>) were measured directly. Horizontal lines are the correct CO<sub>2</sub>  
 138 concentrations. Uncertainties in the estimates correspond to the 16<sup>th</sup>-84<sup>th</sup> percentile range. Circles are  
 139 from Londoño et al. (2018), squares from Milligan et al. (2019), large triangle from Maxbauer et al.  
 140 (2014), small triangles from Kowalczyk et al. (2018), and diamonds from Franks et al. (2014).

141  
 142

143 In these studies, two of the key physiological inputs were measured directly with an infrared gas  
 144 analyzer: the assimilation rate at a known CO<sub>2</sub> concentration ( $A_0$ ) and/or the ratio of operational to  
 145 maximum stomatal conductance to CO<sub>2</sub> ( $g_{c(op)}/g_{c(max)}$ ), or  $\zeta$ , the latter of which is important for  
 146 calculating the total leaf conductance ( $g_{c(tot)}$ ). These two inputs cannot be directly measured on fossils;  
 147 thus, the error rates associated with Figure 1 may not be representative for fossil studies. Franks et al.  
 148 (2014) argue that within plant functional types growing in their natural environment, mean  $A_0$  is fairly  
 149 conservative, leading to the recommended mean  $A_0$  values in Franks et al. (2014) (12  $\mu\text{mol m}^{-2} \text{s}^{-1}$  for  
 150 angiosperms, 10 for conifers, and 6 for ferns and ginkgos). Along similar lines, the mean ratio  $g_{c(op)}/g_{c(max)}$   
 151 tends to be conserved across plant functional types; Franks et al. (2014) recommend a value of 0.2,  
 152 which may correspond to the most efficient setpoint for stomata to control conductance (Franks et al.,  
 153 2012). This conservation of physiological function is one of the underlying principles in the Franks  
 154 model.

155 Here we test this assumption by estimating CO<sub>2</sub> from 40 phylogenetically diverse species of  
 156 field-grown trees. In making these estimates, we use the recommended mean values of  $A_0$  and  
 157  $g_{c(op)}/g_{c(max)}$  from Franks et al. (2014) instead of measuring them directly (see also Montañez et al., 2016  
 158 for other ways to infer assimilation rate from fossils). Thus, this dataset should be a more faithful gauge

159 for model accuracy as applied to fossils. Of the 40 species, 21 were previously published in Londoño et  
160 al. (2018), who collected sun-adapted canopy leaves of angiosperms using a crane in Parque Nacional  
161 San Lorenzo, Panama. To test the method in temperate forests, we collected leaves from eleven  
162 angiosperm and seven conifer species from Dinosaur State Park (Rocky Hill, Connecticut), Wesleyan  
163 University (Middletown, Connecticut), and Connecticut College (New London, Connecticut) during the  
164 summer of 2015. Here, all trees grew in open, park-like settings; one to three sun leaves were sampled  
165 from the lower outside crown of each tree. In January of 2015, we also sampled sun-exposed leaves  
166 from the tree fern *Cyathea arborea* in El Yunque National Forest, Puerto Rico (near the Yokahú Tower).

167 Stomatal size and density were measured either on untreated leaves using epifluorescence  
168 microscopy with a 420-490 nm filter, or on cleared leaves (using 50% household bleach or 5% NaOH)  
169 using transmitted-light microscopy. For most species, whole-leaf  $\delta^{13}\text{C}$  comes from Royer and Hren  
170 (2017); the same leaves were measured for  $\delta^{13}\text{C}$  and stomatal morphology. The UC Davis Stable Isotope  
171 Facility measured some additional leaf samples. Atmospheric CO<sub>2</sub> concentration (400 ppm) and  $\delta^{13}\text{C}_{\text{air}}$  (-  
172 8.5‰) come from Mauna Loa, Hawaii (NOAA/ESRL, 2019), which we assume are representative of the  
173 local conditions where we sampled (e.g., Munger and Hadley, 2017). Table S1 summarizes for these 40  
174 species all of the inputs needed to run the Franks model, along with the estimated CO<sub>2</sub> concentrations.  
175 Uncertainties in the estimates are based on error propagation using Monte Carlo simulations (Franks et  
176 al., 2014).

177

## 178 2.2 Temperature

179

180 The Franks model can be configured for any temperature. Franks et al. (2014) recommend that the  
181 photosynthesis parameters  $A_0$  and  $\Gamma^*$ , and the air physical properties affecting diffusion of CO<sub>2</sub> into the  
182 leaf (the ratio of CO<sub>2</sub> diffusivity in air to the molar volume of air, or  $d/v$ ) correspond with the mean  
183 daytime growing-season leaf temperature (more precisely, assimilation-weighted leaf temperature). The  
184 reasoning behind this is that (i) the assimilation-weighted leaf temperature corresponds with the mean  
185  $c/c_a$  derived from fossil leaf  $\delta^{13}\text{C}$ ; and (ii) both theory (Michaletz et al., 2015, 2016) and observations  
186 (Helliker and Richter, 2008; Song et al., 2011) indicate that the control of leaf gas exchange leads to  
187 relatively stable assimilation-weighted leaf temperatures (~19-25 °C from temperate to tropical regions)  
188 despite large differences in air temperature. This is mostly due to the effects of transpiration on leaf  
189 energy balance. Franks et al. (2014) chose a fixed temperature of 25 °C because much of the Mesozoic  
190 and Cenozoic correspond to climates warmer than the present-day. When applying the Franks model to  
191 known cooler paleoenvironments, improved accuracy may be achieved with leaf-temperature-  
192 appropriate values for  $A_0$ ,  $\Gamma^*$ , and  $d/v$ .

193 Bernacchi et al. (2003) proposed the following temperature sensitivity for  $\Gamma^*$  based on  
194 experiments:

195

$$196 \Gamma^* = e^{(19.02 - \frac{37.83}{RT})}, \quad (6)$$

197

198 where  $R$  is the molar gas constant ( $8.31446 \times 10^{-3}$  kJ K<sup>-1</sup> mol<sup>-1</sup>) and  $T$  is leaf temperature (K). Marrero and  
199 Mason (1972) describe the sensitivity of water vapor diffusivity to temperature as:

200

$$201 d = 1.87 \times 10^{-10} \left( \frac{T^{2.072}}{P} \right), \quad (7)$$

202

203 where  $P$  is atmospheric pressure, which we fix at 1 atmosphere. Lastly, the temperature sensitivity of  
204 the molar volume of air follows ideal gas principles:

205

206  $v = v_{STP} \left( \frac{T}{T_{STP}} \right) \left( \frac{P}{P_{STP}} \right)$ , (8)

207

208 where  $T_{STP}$  is 273.15 K,  $P_{STP}$  is 1 atmosphere, and  $v_{STP}$  is the air volume at  $T_{STP}$  and  $P_{STP}$  ( $0.022414 \text{ m}^3 \text{ mol}^{-1}$ ).

210 Using Eqs. (6-8), we can describe how, conceptually, the sensitivities of  $\Gamma^*$  and  $d/v$  to leaf  
 211 temperature affect estimates of  $\text{CO}_2$  from the Franks model. We apply these relationships to a suite of  
 212 409 fossil and extant leaves from 62 species of angiosperms, gymnosperms, and ferns. These data come  
 213 from the current study (see Sect. 2.1 and 2.4) and Londoño et al. (2018), Kowalczyk et al. (2018), and  
 214 Milligan et al. (2019).

215 To experimentally test more generally how the Franks model is influenced by temperature, we  
 216 grew six species of plants inside two growth chambers with contrasting temperatures (Conviron E7/2;  
 217 Winnipeg, Canada). Air temperature was  $28 \pm 0.5^\circ\text{C}$  ( $1\sigma$ ) and  $20 \pm 0.3^\circ\text{C}$  during the day, and  $19 \pm 0.7^\circ\text{C}$   
 218 and  $11 \pm 1.1^\circ\text{C}$  during the night. We note that the difference in leaf temperature was probably smaller  
 219 than that in air temperature during the day ( $8^\circ\text{C}$ ; see earlier discussion). We held fixed the day length  
 220 (17 hours with a 30 minute simulated dawn and dusk) and  $\text{CO}_2$  concentration ( $500 \pm 10 \text{ ppm}$ ). Light  
 221 intensity at the heights where we sampled leaves ranged from  $100\text{-}400 \mu\text{mol m}^{-2} \text{ s}^{-1}$ . Humidity differed  
 222 moderately between chambers ( $76.5 \pm 1.8\%$  and  $90.0 \pm 3.6\%$ ). To minimize any chamber effects, we  
 223 alternated plants between chambers every two weeks.

224 Four of the species started as saplings purchased from commercial nurseries: bare-root, one-  
 225 foot tall saplings of *Acer negundo* and *Carpinus caroliniana*, one-foot tall saplings of *Ostrya virginiana*  
 226 with a soil ball, and bare-root, four-inch tall saplings of *Ilex opaca*. We grew the other two species from  
 227 seed: *Betula lenta* from a commercial source, and *Quercus rubra* from a single tree on Wesleyan  
 228 University's campus. All seeds were soaked in water for 24 hours and then cold stratified in a  
 229 refrigerator for 30 and 60 days, respectively.

230 All seeds and saplings grew in the same potting soil (Promix Bx with Mycorise; Premier  
 231 Horticulture; Quakertown, Pennsylvania, USA) and fertilizer (Scotts all-purpose flower and vegetable  
 232 fertilizer; Maryville, Ohio, USA). They were watered to field capacity every other day, and we discarded  
 233 any excess water passing through the pots. After three months of growth in the chambers, for each  
 234 species-chamber pair we harvested the three newest fully expanded leaves whose buds developed  
 235 during the experiment. In most cases, we harvested five plants per species-chamber pair; the one  
 236 exception was *I. opaca*, where we were limited to three plants in the warm treatment and two in the  
 237 cool treatment.

238 We measured stomatal size and density on cleared leaves (using 50% household bleach) with  
 239 transmitted-light microscopy. Whole-leaf  $\delta^{13}\text{C}$  comes from the UC Davis Stable Isotope Facility and the  
 240 Light Stable Isotope Mass Spec Lab at the University of Florida; the same leaves were measured for  $\delta^{13}\text{C}$   
 241 and stomatal morphology. We used either a hole punch or razor to remove two adjacent sections of leaf  
 242 tissue near the leaf centers, avoiding major veins. Because we used the same  $\text{CO}_2$  gas cylinder ( $\delta^{13}\text{C} = -$   
 243  $11.8\text{\textperthousand}$ ) and laboratory space ( $\delta^{13}\text{C} = -10.4\text{\textperthousand}$ ) as Milligan et al. (2019), we used their two-end-member  
 244 mixing model ( $1/\text{CO}_2$  vs.  $\delta^{13}\text{C}$ ; Keeling, 1958) to calculate the  $\delta^{13}\text{C}$  of the chamber  $\text{CO}_2$  at 500 ppm (-10.6  
 245  $\text{\textperthousand}$ ). We used the recommended values from Franks et al. (2014) for the physiological inputs  $A_o$  and  
 246  $g_{c(\text{op})}/g_{c(\text{max})}$ . Table S1 summarizes all of the inputs from this experiment needed to run the Franks model,  
 247 along with the estimated  $\text{CO}_2$  concentrations. The standard errors for the inputs are based on plant  
 248 means.

249 To test if leaf  $\delta^{13}\text{C}$  and stomatal morphology (stomatal density, stomatal pore length, and single  
 250 guard cell width) differed between temperature treatments across species, we implemented a mixed  
 251 model in R (R Core Team, 2016) using the lme4 (Bates et al., 2015) and lmerTest (Kuznetsova et al.,  
 252 2017) packages, with temperature and species as the two fixed factors. To test if there was a significant

253 difference between CO<sub>2</sub> estimates from the two temperature treatments, we ran a Kolmogorov–  
254 Smirnov (KS) test in R. For each species, we first estimated CO<sub>2</sub> for each plant in the warm and cool  
255 treatments based on simulated inputs constrained by their means and variances. In the typical case with  
256 five plants per chamber, this produced five CO<sub>2</sub> estimates for the warm chamber and the same for the  
257 cool chamber. A KS test was then used to test for a significant temperature effect. We repeated this  
258 procedure 10,000 times, with 10,000 associated KS tests. The fraction of tests with a p-value < 0.05 was  
259 taken as the overall p value. An advantage of this approach is that it incorporates both within- and  
260 across-plant variation.

261

262

### 263 2.3 Photorespiration

264

265  $c_i/c_a$  is estimated in the Franks model following Farquhar et al. (1982):

266

$$267 \Delta_{leaf} = a + (b - a) \times \frac{c_i}{c_a}, \quad (9)$$

268

269 where  $a$  is the carbon isotope fractionation due to diffusion of CO<sub>2</sub> in air (4.4‰; Farquhar et al., 1982),  $b$   
270 is the fractionation associated with RuBP carboxylase (30‰; Roeske and O'Leary, 1984), and  $\Delta_{leaf}$  is the  
271 net fractionation between air and assimilated carbon ( $[\delta^{13}\text{C}_{\text{air}} - \delta^{13}\text{C}_{\text{leaf}}]/[1+\delta^{13}\text{C}_{\text{leaf}}/1000]$ ).

272 Equation (9) can be expanded to include other effects, including photorespiration (Farquhar et  
273 al., 1982):

274

$$275 \Delta_{leaf} = a + (b - a) \times \frac{c_i}{c_a} - \frac{f\Gamma^*}{c_a}, \quad (10)$$

276

277 where  $f$  is the carbon isotope fractionation due to photorespiration. Photorespiration occurs when the  
278 enzyme rubisco fixes O<sub>2</sub>, not CO<sub>2</sub> (i.e., RuBP oxygenase). One product of photorespiration is CO<sub>2</sub> (Jones,  
279 1992), whose δ<sup>13</sup>C is lower than the source substrate glycine. If this respired CO<sub>2</sub> escapes to the  
280 atmosphere, the δ<sup>13</sup>C of the leaf carbon becomes more positive. Thus, if  $c_i/c_a$  is calculated using Eq. (9),  
281 as is common practice, the calculation may be falsely low, leading to an underprediction of atmospheric  
282 CO<sub>2</sub>.

283 Measured values for  $f$  vary from ~9–15‰ (see compilation in Schubert and Jahren, 2018), which  
284 is in line with theoretical predictions (Tcherkez, 2006). At a 400 ppm atmospheric CO<sub>2</sub> and  $\Gamma^*$  of 40 ppm,  
285 Eq. (10) implies that ~1‰ of  $\Delta_{leaf}$  is due to photorespiration, meaning that  $c_i/c_a$  should be ~0.04 higher  
286 relative to Eq. (9). Here, using the suite of fossil and extant leaves described in Sect. 2.2, we explore how  
287 the carbon isotopic fractionation associated with photorespiration affects CO<sub>2</sub> estimates with the Franks  
288 model. Because  $c_i/c_a$  is present in both of the fundamental equations (Eqs. 2 and 3), we solve them  
289 iteratively until  $c_i/c_a$  converges.

290

### 291 2.4 Leaves that grow close to the forest floor

292

293 The composition of air close to the forest floor can differ considerably from the well-mixed atmosphere.  
294 Of relevance to the Franks model, soil respiration can lead to a locally higher CO<sub>2</sub> concentration and  
295 lower δ<sup>13</sup>C<sub>air</sub> (Table 2). This effect is strongest at night, when the forest boundary layer is thickest (e.g.,  
296 Munger and Hadley, 2017), but we focus here on daylight hours because that is when most plants take  
297 up CO<sub>2</sub>. In wet tropical forests, which can have very high soil respiration rates, CO<sub>2</sub> during the day near  
298 the forest floor can be elevated by tens-of-pmm, and the δ<sup>13</sup>C<sub>air</sub> can be 2–3‰ lower; in temperate forests,

299 the deviations are smaller (Table 2). Above ~2 m, CO<sub>2</sub> concentrations and air δ<sup>13</sup>C during the daytime  
 300 largely match the well-mixed atmosphere.

301  
 302  
**303 Table 2.** Deviations in the δ<sup>13</sup>C and concentration of CO<sub>2</sub> close to a forest floor relative to well-mixed air  
 304 above the canopy. All measurements were made close to mid-day.

<b>Study</b>	<b>δ<sup>13</sup>C<sub>air</sub> relative to well-mixed air (‰)</b>	<b>CO<sub>2</sub> relative to well-mixed air (ppm)</b>	<b>Height above forest floor (m)</b>	<b>Forest location</b>
<b>Tropical forest</b>				
Broadmeadow et al. (1992)	-2	+20	0.15-1	Trinidad during dry season
Buchmann et al. (1997)	-2	+30	0.70-0.75	French Guiana during wet and dry seasons
Holtum and Winter (2001)	NA	+50	0.10	Panama during wet and dry seasons
Lloyd et al. (1996)	-3	+70	1	Brazil (Amazon Basin)
Quay et al. (1989)	-3	+20	2	Brazil (Amazon Basin)
Sternberg et al. (1989)	-2	+25	1	Panama during wet and dry seasons
<b>Temperate forest</b>				
Francey et al. (1985)	-1	+20	1	Tasmania
Munger and Hadley (2017)	NA	+15	1	Massachusetts (Harvard Forest)

305  
 306  
 307 As a result, leaves that grow close to the forest floor may cause the Franks model to produce  
 308 CO<sub>2</sub> estimates higher than that of the mixed atmosphere for at least two reasons. First, the  
 309 concentration of CO<sub>2</sub> near the forest floor is elevated; that is, the model may correctly estimate a CO<sub>2</sub>  
 310 concentration that the user is not interested in. Second, because the δ<sup>13</sup>C<sub>air</sub> that a forest-floor plant  
 311 experiences is lower than the global well-mixed value, if the user chooses the well-mixed value for  
 312 model input (inferred, for example, from the δ<sup>13</sup>C of marine carbonate; Tipple et al., 2010), then c<sub>i</sub>/c<sub>a</sub>  
 313 and thus atmospheric CO<sub>2</sub> will be overestimated (see Eq. 2).

314 We sought to test how the Franks model is affected by the forest-floor microenvironment for  
 315 five tropical angiosperm species and fifteen temperate angiosperm and fern species. The tropical leaves  
 316 were sampled at ~1-2 m height from Parque Nacional San Lorenzo, Panama. In contrast to the canopy  
 317 data set from San Lorenzo (Sect. 2.1), these CO<sub>2</sub> estimates have not been previously reported. In the  
 318 summer of 2015, seven fern species were sampled at ~0.5 m height from Connecticut College and  
 319 Wesleyan University. Also, we used leaf vouchers from Royer et al. (2010), who sampled eight  
 320 herbaceous angiosperm species at ~0.1-0.2 m height from Reed Gap, Connecticut. For all 20 species,  
 321 stomatal and carbon isotopic measurements follow the methods described in Sect. 2.1. Table S1  
 322 contains all of the inputs needed to run the Franks model, along with the estimated CO<sub>2</sub> concentrations.

323 We also investigated if we could include the forest-floor δ<sup>13</sup>C<sub>air</sub> effect in our estimates of  
 324 atmospheric CO<sub>2</sub>. We did not measure the CO<sub>2</sub> concentration and δ<sup>13</sup>C<sub>air</sub> around our plants, so we could  
 325 not directly compare our values. But, if the only CO<sub>2</sub> inputs close to the forest floor are from the soil and  
 326 well-mixed atmosphere, then the system can be modeled as a two-endmember mixing model where

327  $\delta^{13}\text{C}_{\text{air}}$  has a positive, linear relationship with  $1/\text{CO}_2$  (Keeling, 1958). If the  $\text{CO}_2$  concentration and  $\delta^{13}\text{C}$  of  
328 both endmembers are known, the forest-floor microenvironment should fall somewhere on the  
329 modelled line. Importantly, the Franks model provides a second constraint on the system. Here,  $\delta^{13}\text{C}_{\text{air}}$   
330 has a negative, nonlinear relationship with  $1/\text{CO}_2$  because  $\delta^{13}\text{C}_{\text{air}}$  is positively related to  $c_i/c_a$  and  $\text{CO}_2$ .  
331 The Franks model thus provides a second calculation for the relationship between  $\delta^{13}\text{C}_{\text{air}}$  and estimated  
332  $\text{CO}_2$  concentration. The intersection between the two curves should be the correct  $\delta^{13}\text{C}_{\text{air}}$  and  $\text{CO}_2$   
333 concentration for the forest-floor microenvironment.

334 To estimate the soil  $\text{CO}_2$  endmember, we measured the  $\delta^{13}\text{C}$  of soil organic matter collected  
335 from the A horizons of 13 soil sites at San Lorenzo, and of five each at Reed Gap and Connecticut  
336 College. For all soils, we assume a 5000 ppm  $\text{CO}_2$  concentration for a depth that is below the zone of  $\text{CO}_2$   
337 diffusion from the atmosphere ( $\sim 0.3$  m; Cerling, 1999; Breecker et al., 2009). The true value for wet  
338 temperate and tropical forest soils may be somewhat less or substantially more than 5000 ppm (Medina  
339 et al., 1986; Cerling, 1999; Hirano et al., 2003; Hashimoto et al., 2004; Sotta et al., 2004). Because the  
340 mixing model uses  $1/\text{CO}_2$ , a much higher  $\text{CO}_2$  concentration (e.g., 10000 ppm) has little impact on our  
341 results.

342

343

### 344 **3 Results and Discussion**

345

#### 346 3.1 General testing in living plants

347

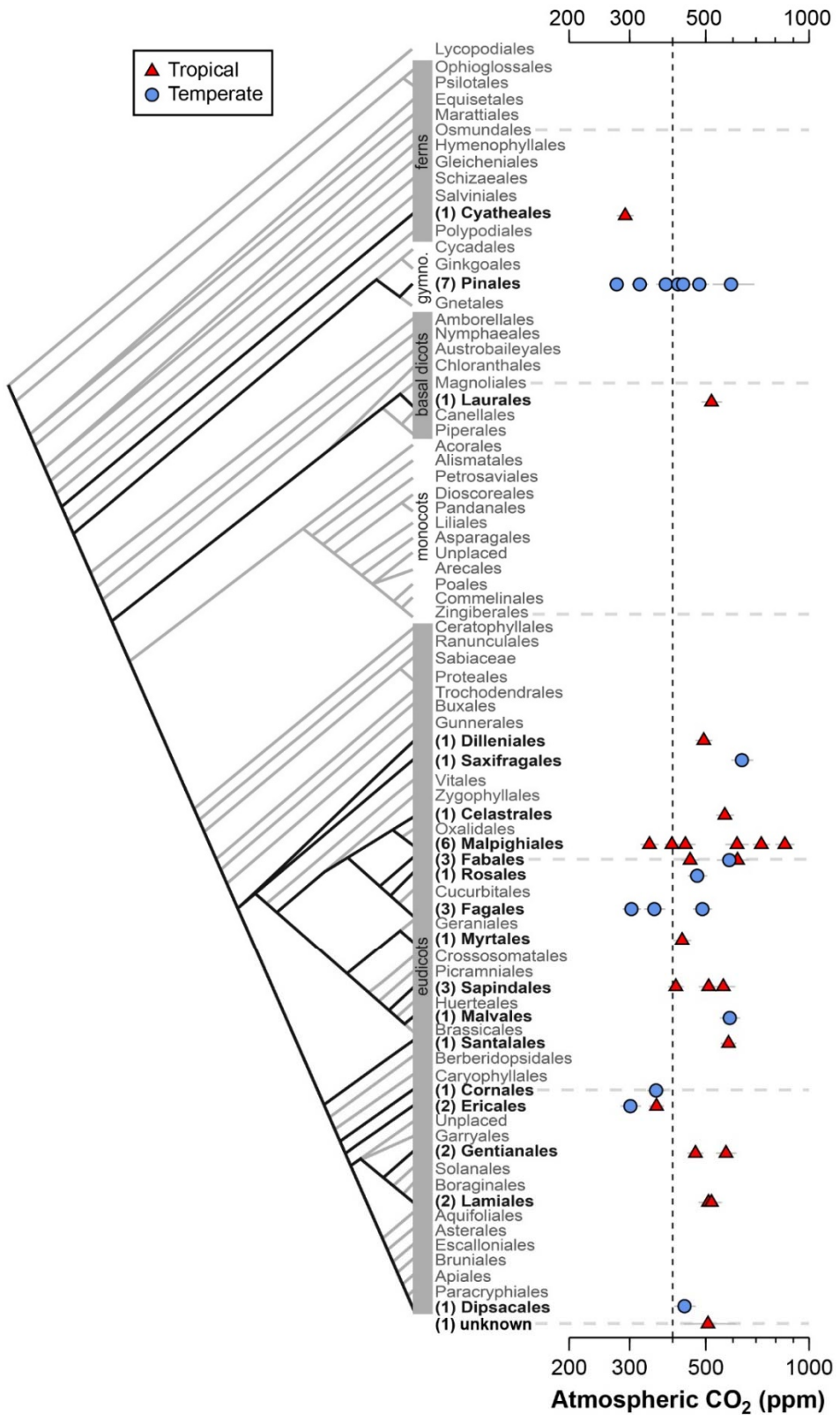
348 Estimates of  $\text{CO}_2$  across the 40 tree species sampled in the field range from 275 to 850 ppm, with a  
349 mean of 478 ppm and median of 472 ppm (Fig. 2); two-thirds of the estimates (a close equivalent to  $\pm 1$   
350 standard deviation) range between 353 and 585 ppm. In 28% of the tested species, the estimated  $\text{CO}_2$   
351 concentrations overlap with the target concentration (400 ppm) at 95% confidence; for these species,  
352 the  $\text{CO}_2$  estimates do not differ significantly from the target. There are no strong differences across  
353 taxonomic orders, nor between leaves from tropical and temperate forests. The mean error rate across  
354 the estimates is 28% (median = 24%), which is higher than estimates that include direct measurements  
355 of the physiological inputs  $A_0$  and  $g_{c(\text{op})}/g_{c(\text{max})}$  (mean = 20%; median = 13%; Fig. 1). Along similar lines, if  
356 the estimates presented in Fig. 1 are re-estimated using the values for  $A_0$  and  $g_{c(\text{op})}/g_{c(\text{max})}$  recommended  
357 by Franks et al. (2014), the mean error rate increases to 37% (median = 33%). If only the default values  
358 of  $A_0$  are used, the median error rate is 27%; and for only default values of  $g_{c(\text{op})}/g_{c(\text{max})}$ , 22%.

359 These results indicate that  $\text{CO}_2$  accuracy is generally improved when  $A_0$  and/or  $g_{c(\text{op})}/g_{c(\text{max})}$  is  
360 measured. These measurements require expensive gas-exchange equipment and are not always easy or  
361 practical to make. Moreover,  $A_0$  and  $g_{c(\text{op})}/g_{c(\text{max})}$  cannot be measured on fossils. Some gains in accuracy  
362 are possible by measuring  $A_0$  and  $g_{c(\text{op})}/g_{c(\text{max})}$  on extant relatives of the fossil species (e.g., the same  
363 genus). Absent of this, our analysis using the recommended mean values of Franks et al. (2014) indicates  
364 an error rate, on average, of approximately 28%. This is comparable to or better than other leading  
365 paleo- $\text{CO}_2$  proxies (Franks et al., 2014).

366 One reliable way to improve accuracy is to estimate  $\text{CO}_2$  with multiple species because the  
367 falsely-high and falsely-low estimates partly cancel each other out. The grand mean of estimates  
368 presented in Fig. 2 (478 ppm) is 20% from the 400 ppm target, which is less than the 28% mean error  
369 rate of individual estimates.

370

371



372

373

374

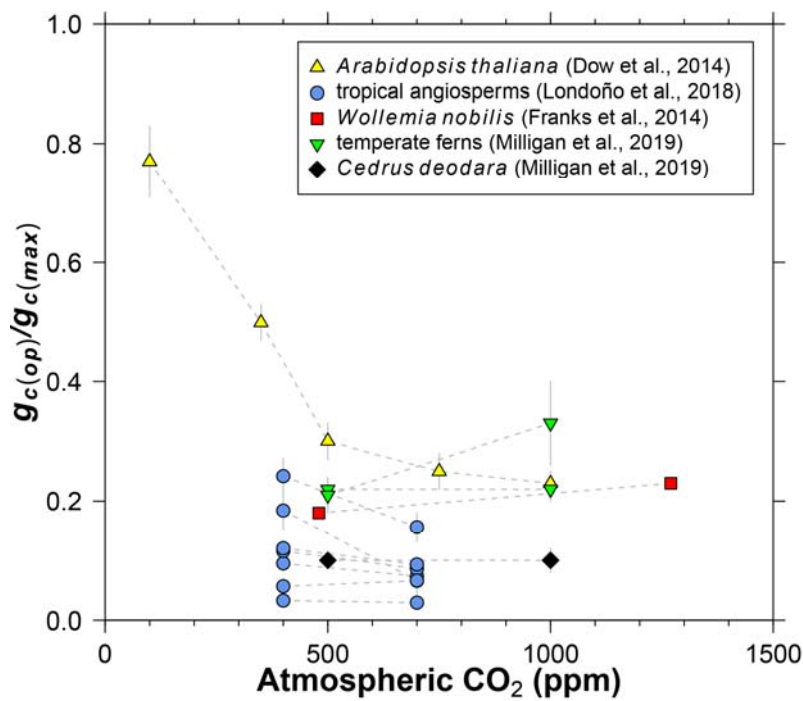
375

**Figure 2.** Estimates of CO<sub>2</sub> based on canopy leaves from 40 tree species. Uncertainties in the estimates correspond to the 16<sup>th</sup>-84<sup>th</sup> percentile range. Vertical line is the correct concentration (400 ppm). On the left is an order-level vascular plant phylogeny (APW v.13; Stevens, 2001 onwards).

376  
377

378 Dow et al. (2014) observed that  $g_{c(op)}/g_{c(max)}$  inversely varies with CO<sub>2</sub> in *Arabidopsis thaliana*, but  
379 primarily at subambient concentrations (yellow triangles in Fig. 3). At elevated CO<sub>2</sub>,  $g_{c(op)}/g_{c(max)}$  is close  
380 to 0.2, which is the value recommended by Franks et al. (2014). Data from eleven species of  
381 angiosperms, conifers, and ferns at present-day (or near present-day) and elevated CO<sub>2</sub> concentrations  
382 support the view of a limited effect at high CO<sub>2</sub> (Fig. 3; Franks et al., 2014; Londoño et al., 2018; Milligan  
383 et al., 2019). More data at subambient CO<sub>2</sub> are needed, but for CO<sub>2</sub> concentrations similar to or higher  
384 than the present-day, we see no strong reason to include a CO<sub>2</sub> sensitivity in  $g_{c(op)}/g_{c(max)}$ . The rather low  
385 values for *Cedrus deodara* and many of the tropical angiosperms (<0.1) are likely due to stress imposed  
386 by their growth chamber environment; these  $g_{c(op)}/g_{c(max)}$  values are probably not representative of field-  
387 grown trees, which tend to be closer to 0.2 (Franks et al., 2014).

388  
389



390  
391  
392

**Figure 3.** Literature compilation of the sensitivity of  $g_{c(op)}/g_{c(max)}$  (ratio of operational to maximum leaf conductance to CO<sub>2</sub>) to atmospheric CO<sub>2</sub> concentration.

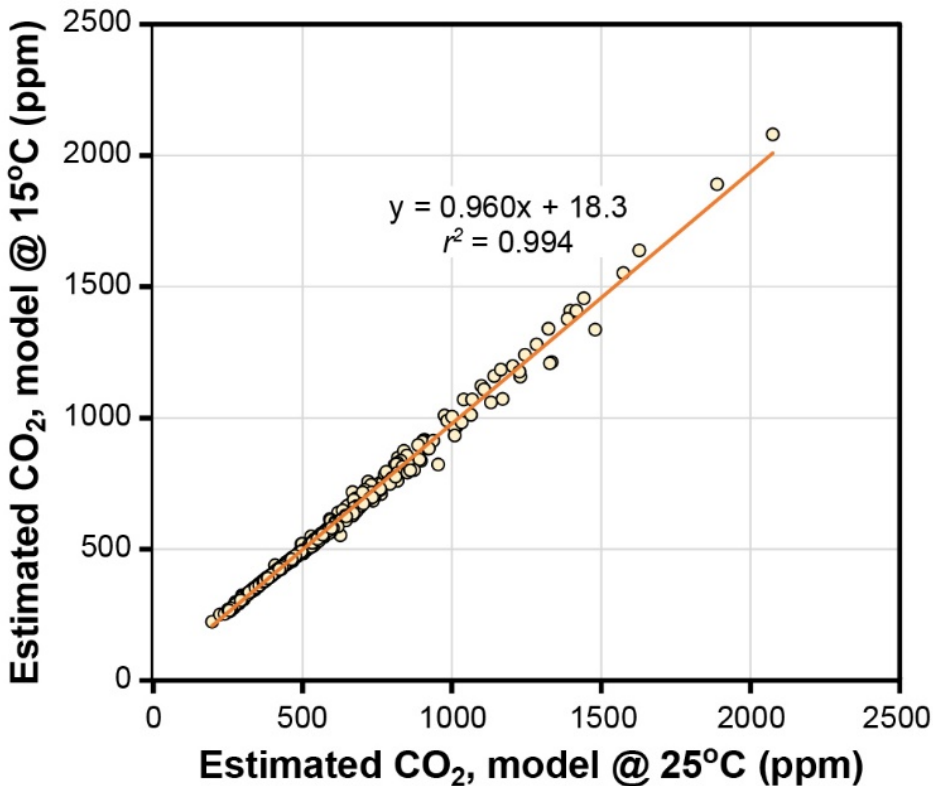
393  
394

### 395 3.2 Temperature

396

397 The temperature sensitivities of the ratio of diffusivity of CO<sub>2</sub> in air to the molar volume of air ( $d/v$ ) and  
398 the CO<sub>2</sub> compensation point in the absence of dark respiration ( $\Gamma^*$ ) have little effect on estimated CO<sub>2</sub> in  
399 the Franks model (Fig. 4). Given that assimilation-weighted leaf temperature only varies about 7 °C  
400 across plants today, the differences shown in Fig. 4—which are based on leaf temperatures of 25 °C and  
401 15 °C—are likely a maximum effect. As such, we consider the use of a fixed leaf temperature (e.g., 25 °C)  
402 in the model to be a defensible simplification.

403  
404



405  
406 **Figure 4.** Estimates of CO<sub>2</sub> at leaf temperatures of 25 °C and 15 °C. Each symbol is an extant or fossil leaf.  
407 The difference in estimated CO<sub>2</sub> for any leaf is due to the theoretical effects of temperature on gas  
408 diffusion ( $d/v$ ) and the CO<sub>2</sub> compensation point in the absence of dark respiration ( $\Gamma^*$ ) (Eqs. 6-8).  
409  
410

411 Other inputs in the model may respond to temperature, though. In our growth chamber  
412 experiments where daytime air temperatures were 28 °C and 20 °C, the effect on estimated CO<sub>2</sub> was  
413 mixed (Fig. 5). In five out of six species, estimated CO<sub>2</sub> was higher in the warm treatment, but for all  
414 species these differences were not statistically significant ( $P > 0.05$  based on a KS test; see Methods).  
415 Incorporating the temperature sensitivities in  $d/v$  and  $\Gamma^*$  had little effect ("adj" estimates in Fig. 5), as  
416 expected from Fig. 4.

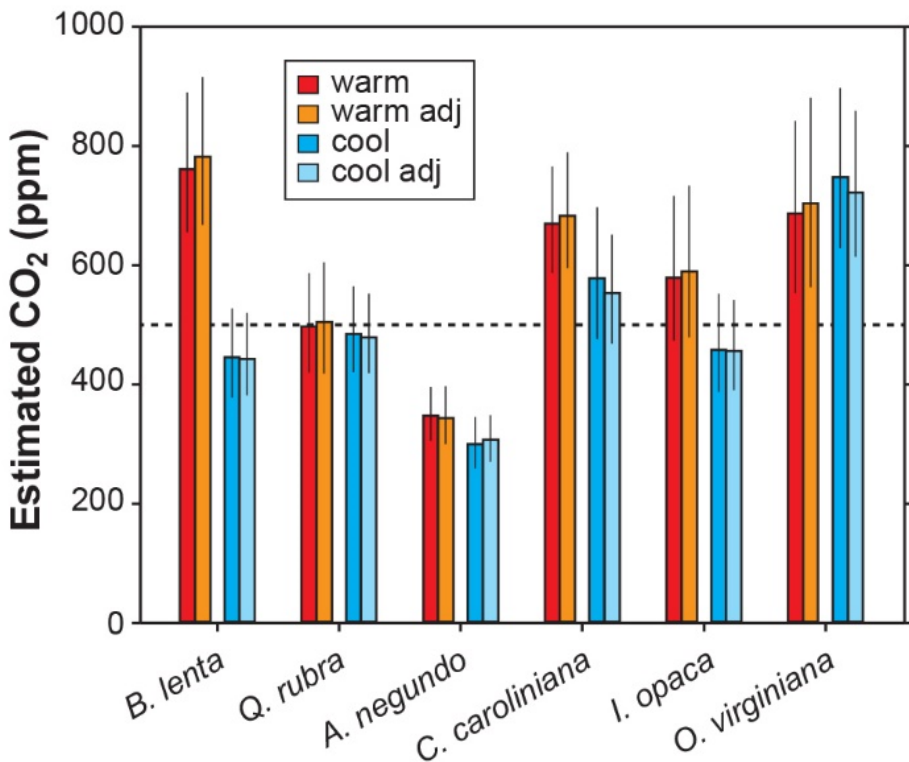
417 None of the measured inputs—stomatal density, stomatal pore length, single guard cell width,  
418 and leaf δ<sup>13</sup>C—were significantly affected by temperature across all species ( $P > 0.05$  for each of the four  
419 inputs based on a mixed model; see Methods). These small differences probably cannot account for the  
420 differences in estimated CO<sub>2</sub> between temperatures. It is more likely that some of the inputs that we did  
421 not directly measure, such as assimilation rate ( $A_0$ ), the  $g_{c(op)}/g_{c(max)}$  ratio, or mesophyll conductance ( $g_m$ ),  
422 differ from the true mean value. In the cases for the five species where estimated CO<sub>2</sub> is higher in the  
423 warm treatment, our mean  $A_0$  for the warm plants must be falsely high, or  $g_{c(op)}/g_{c(max)}$  or  $g_m$  falsely low.

424 In summary, we see no strong reason to expand the parameterization of temperature in the  
425 model, though more growth-chamber experiments may be warranted. We note that in three out of the  
426 six species from the warm treatment, the estimated CO<sub>2</sub> cannot be distinguished from the 500 ppm  
427 target at 95% confidence; for the cool treatment, this is true for four of the species. Also, the across-  
428 species means of estimated CO<sub>2</sub> for the warm and cool treatments are reasonably close to the target  
429 (590 and 502 ppm, respectively) and overall have a mean error rate of 25%. This level of uncertainty is  
430 similar to our field estimates where we did not measure  $A_0$  or  $g_{c(op)}/g_{c(max)}$  (28%; see Fig. 2). This too

431 provides support for our recommendation that it is not critical to include a broader treatment of  
432 temperature in the model.

433

434



435  
436 **Figure 5.** Estimates of CO<sub>2</sub> for plants grown inside growth chambers at daytime air temperatures of 28 °C  
437 and 20 °C. Also shown are estimates after taking into account the temperature sensitivity of gas  
438 diffusion ( $d/v$ ) and the CO<sub>2</sub> compensation point in the absence of dark respiration ( $\Gamma^*$ ) ("adj"; see also  
439 Fig. 4). Dashed line is the correct CO<sub>2</sub> concentration (500 ppm). Uncertainties in the estimates  
440 correspond to the 16<sup>th</sup>-84<sup>th</sup> percentile range.

441

442

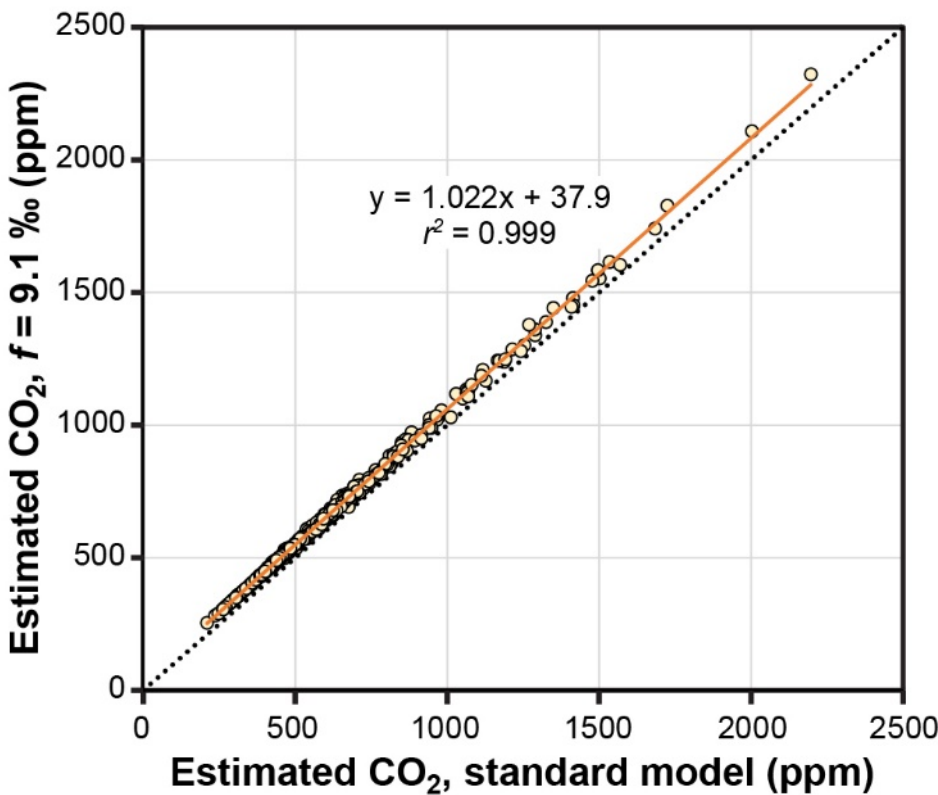
### 443 3.3 Photorespiration

444

445 The theoretical effects of photorespiration do not strongly impact estimates of CO<sub>2</sub> in the Franks model.  
446 The average effect for our 409 extant and fossil leaves is to increase estimated CO<sub>2</sub> by 2.2% plus 38 ppm  
447 (Fig. 6). At 1000 ppm, for example, estimates would increase by 60 ppm. This calculation assumes a  
448 photorespiration fractionation ( $f$ ) of 9.1‰, which is the value estimated for *Arabidopsis thaliana*  
449 (Schubert and Jahren, 2018). If a fractionation towards the upper bound of published estimates is used  
450 instead (15‰), estimated CO<sub>2</sub> increases on average by 3.8% plus 61 ppm. Across this range in  $f$ , the  
451 associated uncertainty in estimated CO<sub>2</sub> is well within the method's overall precision (~+35/-25% at 95%  
452 confidence; Franks et al., 2014). As such, CO<sub>2</sub> estimates made without these photorespiration effects  
453 (i.e. using Eq. 9 instead of Eq. 10) should be reliable, although some improvement is possible using Eq.  
454 10 in cases where  $f$  is accurately known.

455

456



457  
458 **Figure 6.** Estimates of CO<sub>2</sub> with and without a photorespiration effect ( $f = 9.1\text{\textperthousand}$ ; see Eq. 10). Each  
459 symbol is an extant or fossil leaf. Dashed line is  $y=x$ .  
460  
461

462 We note that both  $f$  and  $\Gamma^*$  are also affected by atmospheric O<sub>2</sub> concentration. Because O<sub>2</sub> is  
463 directly responsible for photorespiration,  $f$  should scale with O<sub>2</sub> (or, more precisely, the O<sub>2</sub>:CO<sub>2</sub> molar  
464 ratio). Unfortunately, this effect is poorly constrained (Beerling et al., 2002; Berner et al., 2003; Porter et  
465 al., 2017). In contrast, the theoretical effect of O<sub>2</sub> on  $\Gamma^*$  is known: it is linear with an approximate slope  
466 of 2 (Farquhar et al., 1982; see their Eq. B13). During the Phanerozoic, O<sub>2</sub> likely ranged from 10-30%,  
467 with lows during the early Paleozoic and early Triassic, and highs during the Carboniferous to early  
468 Permian and Cretaceous (Berner, 2009; Glasspool and Scott, 2010; Arvidson et al., 2013; Mills et al.,  
469 2016; Lenton et al., 2018). Assuming a present-day  $\Gamma^*$  of 40 ppm (at 21% O<sub>2</sub>),  $\Gamma^*$  would be 60 ppm at  
470 30% O<sub>2</sub> and 20 ppm at 10% O<sub>2</sub>. Running the Franks model on our library of 409 extant and fossil leaves,  
471 we find little effect on estimated CO<sub>2</sub>: estimates are 7.4% higher on average at 30% O<sub>2</sub> than at 10% O<sub>2</sub>  
472 (see also McElwain et al., 2016).

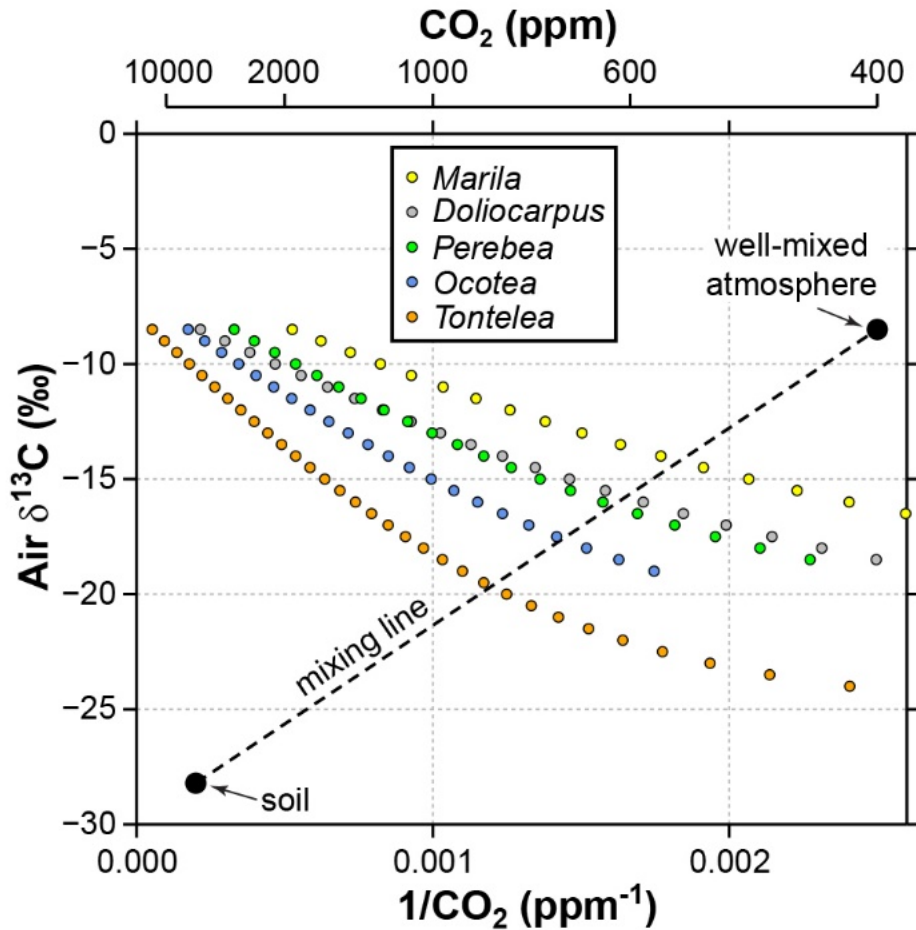
473  
474 3.4 Leaves that grow close to the forest floor  
475

476 CO<sub>2</sub> estimates for tropical understory leaves from five species at San Lorenzo, Panama, are very high,  
477 ranging from 1903 to 18863 ppm (species mean = 6837 ppm). For two of the species, Londoño et al.  
478 (2018) also analyzed canopy leaves from trees nearby, and these within-species comparisons highlight  
479 the vast discrepancy (*Ocotea* sp.: 541 vs. 5737 ppm; *Tontelea* sp.: 622 vs. 18863 ppm). The primary  
480 difference in the inputs between the canopy and understory leaves is the  $\delta^{13}\text{C}_{\text{leaf}}$ : Londoño et al. (2018)  
481 report a species-mean  $\delta^{13}\text{C}_{\text{leaf}}$  of -30.0‰ for the 21 canopy species versus -35.6‰ for the five understory

482 species. This difference leads to very different mean estimates of  $c_i/c_a$ : 0.69 for canopy leaves versus a  
 483 highly unrealistic (Diefendorf et al., 2010) 0.93 for understory leaves.

484 It is likely that the high CO<sub>2</sub> estimates from understory leaves are mostly driven by falsely high  
 485 δ<sup>13</sup>C<sub>air</sub> inputs. Following the mixing model strategy outlined in Sect. 2.4 (and based on a soil organic  
 486 matter δ<sup>13</sup>C of -28.2‰ measured at San Lorenzo), we calculate a species-mean δ<sup>13</sup>C<sub>air</sub> of -16.7‰ (mean  
 487 of intersection points in Fig. 7). When this δ<sup>13</sup>C<sub>air</sub> is used to estimate CO<sub>2</sub> with the Franks model (instead  
 488 of -8.5‰), the species mean drops to 699 ppm. This is somewhat higher than the species mean from  
 489 canopy leaves in the same forest (563 ppm; red triangles in Fig. 2; Londoño et al., 2018).

490  
 491



492  
 493 **Figure 7.** Sensitivity of estimated CO<sub>2</sub> in the Franks model to the δ<sup>13</sup>C of atmospheric CO<sub>2</sub>. Estimates  
 494 come from leaves of five angiosperm species that grew close to the forest floor in Parque Nacional San  
 495 Lorenzo, Panama. The step in δ<sup>13</sup>C<sub>air</sub> between estimates is 0.5‰. The dashed line is a two-endmember  
 496 mixing model for CO<sub>2</sub> between the soil and well-mixed atmosphere. The intersection between the  
 497 mixing model and the Franks model should correspond to the CO<sub>2</sub> concentration and δ<sup>13</sup>C<sub>air</sub> of the  
 498 forest-floor microenvironment.

499  
 500

501 Understory leaves from Connecticut temperate forests show similar but less dramatic patterns,  
 502 which we attribute to a more open canopy with stronger atmospheric mixing. CO<sub>2</sub> estimates for the 15  
 503 species range from 447 to 1567 ppm (mean = 794 ppm). Our intersection method identifies a mean

504  $\delta^{13}\text{C}_{\text{air}}$  of -11.2‰ for the Wesleyan and Connecticut College campuses (based on a soil  $\delta^{13}\text{C}$  of -27.6‰ measured at Connecticut College) and -10.3‰ for Reed Gap (soil  $\delta^{13}\text{C} = -26.4\text{\textperthousand}$ ). Using these adjusted  $\delta^{13}\text{C}_{\text{air}}$ , the species mean of estimated  $\text{CO}_2$  drops to 566 ppm, which is somewhat higher than the species mean from canopy leaves in the same areas (449 ppm; blue circles in Fig. 2).

508 We acknowledge that this analysis is too simple. First, we did not measure the understory  $\text{CO}_2$  concentration and  $\delta^{13}\text{C}_{\text{air}}$  (this would require repeated measurements during different daytime hours over a growing season to calculate a time-integrated value); instead, we assumed a simple two end-member mixing model between the soil and well-mixed atmosphere. Second, other factors probably contribute to the differences in estimated  $\text{CO}_2$  between canopy and understory leaves. Our predicted  $\delta^{13}\text{C}_{\text{air}}$  values are too low (~8‰ and 2‰ lower than the well-mixed atmosphere for the tropical and temperate forests) and our estimated  $\text{CO}_2$  too high (~100 ppm higher than that from canopy leaves). In the lowermost 1-2 meters of the canopy, previous work suggests up to a -3‰ and +70 ppm deviation in tropical forests and -1‰ / +20 ppm in temperate forests (Table 1). One input that could help to resolve this discrepancy is the assimilation rate ( $A_0$ ). We assumed a fixed  $A_0$  of 12  $\mu\text{mol m}^{-2} \text{s}^{-1}$  for all leaves, regardless of canopy position. Shade leaves often have lower assimilation rates than sun leaves (Givnish, 1988). Substituting lower  $A_0$  values for understory leaves would lower estimated  $\text{CO}_2$  roughly in proportion (Eqs. 2-3). Using lower  $A_0$  values for shade leaves in the model is appropriate, but determining the best value is difficult. Typical  $A_0$  values for leaves growing at the top of the canopy in full sun are far more consistent because photosynthesis in these leaves is usually at its maximum capacity (saturated at full sunlight) for the prevailing atmospheric  $\text{CO}_2$  concentration. Because the degree of shadiness near the forest floor is highly variable, photosynthesis ( $A_0$ ) in these leaves will be acclimated to some fraction of the full-sun maximum in a sun exposed leaf, but careful thought must go into determining what this fraction is.

527 We note that our mixing-model strategy cannot be applied to fossils because the global atmospheric  $\text{CO}_2$  concentration is needed (one endpoint for dashed line in Fig. 7). Instead, our motivation for the analysis is to demonstrate that: 1) leaves growing in the lowermost 2 m of the canopy should be considered with caution in the context of the Franks model; and 2) the failure of the model is due to faulty inputs (mostly  $\delta^{13}\text{C}_{\text{air}}$ ), not the model itself.

532 In most fossil leaf deposits, shade morphotypes are comparatively rare (e.g., Kürschner, 1997; Wang et al., 2018) because—relative to sun leaves—they are less durable, do not travel as far by wind, and are produced at a slower rate (Dilcher, 1973; Roth and Dilcher, 1978; Spicer, 1980; Ferguson, 1985; Burnham et al., 1992). Our recommendation is to exclude such leaves. There are several ways to differentiate sun vs. shade morphotypes: overall shape (Talbert and Holch, 1957; Givnish, 1978; Kürschner, 1997; Sack et al., 2006), shape of epidermal cells (larger and with a more undulated outline in shade leaves; Kürschner, 1997; Dunn et al., 2015), vein density (lower in shade leaves; Uhl and Mosbrugger, 1999; Sack and Scoffoni, 2013; Crifò et al., 2014; Londoño et al., 2018), and range in  $\delta^{13}\text{C}_{\text{leaf}}$  (high when both sun and shade leaves are present, for example in our study; Graham et al., 2014). Not all shade leaves grow within 2 m of the forest floor, but excluding all such leaves would eliminate the forest-floor bias.

543

544

#### 545 **4 Conclusions**

546

547 The Franks model is reasonably accurate (~28% error rate) even when the physiological inputs  $A_0$  (assimilation rate at a known  $\text{CO}_2$  concentration) and  $g_{c(\text{op})}/g_{c(\text{max})}$  (ratio of operational to maximum leaf conductance to  $\text{CO}_2$ ) are inferred, not measured. Accuracy does improve when these inputs are measured (~20% error rate), but such measurements are not possible with fossils and may not always

551 be feasible with nearest living relatives. A 28% error rate is broadly in line with (or better than) other  
552 leading paleo-CO<sub>2</sub> proxies.

553 Most of the possible confounding factors that we investigated appear minor. The temperature  
554 sensitivities of  $d/v$  (related to gas diffusion) and  $\Gamma^*$  (CO<sub>2</sub> compensation point in the absence of dark  
555 respiration) have a negligible impact on estimated CO<sub>2</sub>. Our temperature experiments in growth  
556 chambers point to larger differences in some species, which must be related to incorrect values for  
557 inputs that were not directly measured, such as  $A_0$ ,  $g_{c(op)}/g_{c(max)}$ , and  $g_m$  (mesophyll conductance).  
558 Overall, though, we find that the differences in estimated CO<sub>2</sub> imparted by temperature are generally  
559 smaller than the overall 28% error rate.

560 Incorporating the covariance between CO<sub>2</sub> concentration and photorespiration leads to only  
561 small changes in estimated CO<sub>2</sub>. O<sub>2</sub> concentration affects photorespiration and thus may confound CO<sub>2</sub>  
562 estimates from the Franks model, but presently the effect is poorly quantified. The effect of O<sub>2</sub> on  $\Gamma^*$  is  
563 better known, and imparts only small changes in estimated CO<sub>2</sub> across a feasible range in Phanerozoic  
564 O<sub>2</sub> of 10-30%.

565 Leaves from the lowermost 1-2 m of the canopy experience slightly elevated CO<sub>2</sub> concentrations  
566 and lower air  $\delta^{13}\text{C}$  during the daytime relative to the well-mixed atmosphere. We find that if we use the  
567 well-mixed air  $\delta^{13}\text{C}$  to estimate CO<sub>2</sub> from leaves that grew near the forest floor, estimates are too high,  
568 especially in dense tropical canopies. When we use a two-endmember mixing model to calculate the  
569 correct local air  $\delta^{13}\text{C}$ , the falsely-high CO<sub>2</sub> estimates largely disappear. For fossil applications, shade  
570 leaves from the bottom of the canopy should be avoided. Shade leaves are typically rare in the fossil  
571 record (relative to sun leaves), and can be identified by their overall shape, the shape of their epidermal  
572 cells, their low leaf  $\delta^{13}\text{C}$ , and their low vein density.

573 Conceptually, the Franks model holds considerable promise for quantifying paleo-CO<sub>2</sub>: it is  
574 mechanistically grounded and can be applied to most fossil leaves. Our tests of the model's accuracy  
575 and sensitivity to temperature and photorespiration largely uphold this promise.

576  
577  
578 **Author contribution.** DR, KM, MM, and LL designed and conducted the experiments; all authors  
579 interpreted the data; DR prepared the manuscript with contributions from all co-authors.

580  
581 **Competing interests.** The authors declare that they have no conflict of interest.

582  
583 **Acknowledgements.** We thank G. Dreyer and P. Siver for logistical support at Connecticut College, S.  
584 Wang for lab assistance, C. Crifò and A. Baresh for collecting the tropical samples, and J. McElwain, E.  
585 Brook, and an anonymous reviewer for helpful comments. Support for LL was provided by the  
586 Smithsonian Tropical Research Institute; the Mark Tupper Fellowship; National Science Foundation  
587 grants EAR 0824299 and OISE, EAR, DRL 0966884; the Anders Foundation; and the Gregory D. and  
588 Jennifer Walston Johnson and 1923 Fund.

589  
590  
591 **References**

- 592 Arvidson, R. S., Mackenzie, F. T., and Guidry, M. W.: Geologic history of seawater: A MAGic approach to  
593 carbon chemistry and ocean ventilation, *Chemical Geology*, 362, 287-304,  
594 <https://doi.org/10.1016/j.chemgeo.2013.10.012>, 2013.
- 595 Barclay, R. S. and Wing, S. L.: Improving the *Ginkgo* CO<sub>2</sub> barometer: implications for the early Cenozoic  
596 atmosphere, *Earth and Planetary Science Letters*, 439, 158-171,  
597 <https://doi.org/10.1016/j.epsl.2016.01.012>, 2016.

- 598 Bates, D., Mächler, M., Bolker, B., and Walker, S.: Fitting linear mixed-effects models using lme4, Journal  
599 of Statistical Software, 67, <https://doi.org/10.18637/jss.v067.i01>, 2015.
- 600 Beerling, D. J.: Evolutionary responses of land plants to atmospheric CO<sub>2</sub>, in: A History of Atmospheric  
601 CO<sub>2</sub> and Its Effects on Plants, Animals, and Ecosystems, edited by: Ehleringer, J. R., Cerling, T. E.,  
602 and Dearing, M. D., Springer, New York, 114-132, 2005.
- 603 Beerling, D. J., Fox, A., and Anderson, C. W.: Quantitative uncertainty analyses of ancient atmospheric  
604 CO<sub>2</sub> estimates from fossil leaves, American Journal of Science, 309, 775-787,  
605 <https://doi.org/10.2475/09.2009.01>, 2009.
- 606 Beerling, D. J., Lake, J. A., Berner, R. A., Hickey, L. J., Taylor, D. W., and Royer, D. L.: Carbon isotope  
607 evidence implying high O<sub>2</sub>/CO<sub>2</sub> ratios in the Permo-Carboniferous atmosphere, Geochimica et  
608 Cosmochimica Acta, 66, 3757-3767, [https://doi.org/10.1016/S0016-7037\(02\)00901-8](https://doi.org/10.1016/S0016-7037(02)00901-8), 2002.
- 609 Bernacchi, C. J., Pimentel, C., and Long, S. P.: *In vivo* temperature response functions of parameters  
610 required to model RuBP-limited photosynthesis, Plant, Cell & Environment, 26, 1419-1430,  
611 <https://doi.org/10.1046/j.0016-8025.2003.01050.x>, 2003.
- 612 Berner, R. A.: Phanerozoic atmospheric oxygen: new results using the GEOCARBSULF model, American  
613 Journal of Science, 309, 603-606, <https://doi.org/10.2475/07.2009.03>, 2009.
- 614 Berner, R. A., Beerling, D. J., Dudley, R., Robinson, J. M., and Wildman, R. A.: Phanerozoic atmospheric  
615 oxygen, Annual Review of Earth and Planetary Sciences, 31, 105-134,  
616 <https://doi.org/10.1146/annurev.earth.31.100901.141329>, 2003.
- 617 Breecker, D. O., Sharp, Z. D., and McFadden, L. D.: Seasonal bias in the formation and stable isotopic  
618 composition of pedogenic carbonate in modern soils from central New Mexico, USA, Geological  
619 Society of America Bulletin, 121, 630-640, <https://doi.org/10.1130/B26413.1>, 2009.
- 620 Broadmeadow, M., Griffiths, H., Maxwell, C., and Borland, A.: The carbon isotope ratio of plant organic  
621 material reflects temporal and spatial variations in CO<sub>2</sub> within tropical forest formations in  
622 Trinidad, Oecologia, 89, 435-441, <https://doi.org/10.1007/BF00317423>, 1992.
- 623 Buchmann, N., Guehl, J.-M., Barigah, T., and Ehleringer, J. R.: Interseasonal comparison of CO<sub>2</sub>  
624 concentrations, isotopic composition, and carbon dynamics in an Amazonian rainforest (French  
625 Guiana), Oecologia, 110, 120-131, <https://doi.org/10.1007/s004420050140>, 1997.
- 626 Burnham, R. J., Wing, S. L., and Parker, G. G.: The reflection of deciduous forest communities in leaf  
627 litter: implications for autochthonous litter assemblages from the fossil record, Paleobiology, 18,  
628 30-49, <https://doi.org/10.1017/S0094837300012203>, 1992.
- 629 Cerling, T. E.: Stable carbon isotopes in palaeosol carbonates, Special Publications of the International  
630 Association of Sedimentologists, 27, 43-60, 1999.
- 631 Chaloner, W. G. and McElwain, J.: The fossil plant record and global climatic change, Review of  
632 Palaeobotany and Palynology, 95, 73-82, [https://doi.org/10.1016/S0034-6667\(96\)00028-0](https://doi.org/10.1016/S0034-6667(96)00028-0),  
633 1997.
- 634 Crifò, C., Curran, E. D., Baresch, A., and Jaramillo, C.: Variations in angiosperm leaf vein density have  
635 implications for interpreting life form in the fossil record, Geology, 42, 919-922,  
636 <https://doi.org/10.1130/g35828.1>, 2014.
- 637 Diefendorf, A. F., Mueller, K. E., Wing, S. L., Koch, P. L., and Freeman, K. H.: Global patterns in leaf <sup>13</sup>C  
638 discrimination and implications for studies of past and future climate, Proceedings of the  
639 National Academy of Sciences, USA, 107, 5738-5743, <https://doi.org/10.1073/pnas.0910513107>,  
640 2010.
- 641 Dilcher, D. L.: A paleoclimatic interpretation of the Eocene floras of southeastern North America, in:  
642 Vegetation and Vegetational History of Northern Latin America, edited by: Graham, A., Elsevier,  
643 Amsterdam, 39-53, 1973.

- 644 Doria, G., Royer, D. L., Wolfe, A. P., Fox, A., Westgate, J. A., and Beerling, D. J.: Declining atmospheric  
645 CO<sub>2</sub> during the late Middle Eocene climate transition, American Journal of Science, 311, 63-75,  
646 <https://doi.org/10.2475/01.2011.03>, 2011.
- 647 Dow, G. J., Bergmann, D. C., and Berry, J. A.: An integrated model of stomatal development and leaf  
648 physiology, New Phytologist, 201, 1218-1226, <https://doi.org/10.1111/nph.12608>, 2014.
- 649 Dunn, R. E., Strömberg, C. A. E., Madden, R. H., Kohn, M. J., and Carlini, A. A.: Linked canopy, climate,  
650 and faunal change in the Cenozoic of Patagonia, Science, 347, 258-261,  
651 <https://doi.org/10.1126/science.1260947>, 2015.
- 652 Erdei, B., Utescher, T., Hably, L., Tamás, J., Roth-Nebelsick, A., and Grein, M.: Early Oligocene continental  
653 climate of the Palaeogene Basin (Hungary and Slovenia) and the surrounding area, Turkish  
654 Journal of Earth Sciences, 21, 153-186, <https://doi.org/10.3906/yer-1005-29>, 2012.
- 655 Farquhar, G., von Caemmerer, S., and Berry, J.: A biochemical model of photosynthetic CO<sub>2</sub> assimilation  
656 in leaves of C<sub>3</sub> species, Planta, 149, 78-90, <https://doi.org/10.1007/BF00386231>, 1980.
- 657 Farquhar, G. D. and Sharkey, T. D.: Stomatal conductance and photosynthesis, Annual Review of Plant  
658 Physiology, 33, 317-345, <https://doi.org/10.1146/annurev.pp.33.060182.001533>, 1982.
- 659 Farquhar, G. D., O'Leary, M. H., and Berry, J. A.: On the relationship between carbon isotope  
660 discrimination and the intercellular carbon dioxide concentration in leaves, Australian Journal of  
661 Plant Physiology, 9, 121-137, <https://doi.org/10.1071/PP9820121>, 1982.
- 662 Ferguson, D. K.: The origin of leaf-assemblages—new light on an old problem, Review of Palaeobotany  
663 and Palynology, 46, 117-188, [https://doi.org/10.1016/0034-6667\(85\)90041-7](https://doi.org/10.1016/0034-6667(85)90041-7), 1985.
- 664 Francey, R., Gifford, R., Sharkey, T., and Weir, B.: Physiological influences on carbon isotope  
665 discrimination in huon pine (*Lagarostrobos franklinii*), Oecologia, 66, 211-218,  
666 <https://doi.org/10.1007/BF00379857>, 1985.
- 667 Franks, P. J., Leitch, I. J., Ruszala, E. M., Hetherington, A. M., and Beerling, D. J.: Physiological framework  
668 for adaptation of stomata to CO<sub>2</sub> from glacial to future concentrations, Philosophical  
669 Transactions of the Royal Society B, 367, 537-546, <https://doi.org/10.1098/rstb.2011.0270>,  
670 2012.
- 671 Franks, P. J., Royer, D. L., Beerling, D. J., Van de Water, P. K., Cantrill, D. J., Barbour, M. M., and Berry, J.  
672 A.: New constraints on atmospheric CO<sub>2</sub> concentration for the Phanerozoic, Geophysical  
673 Research Letters, 41, 4685-4694, <https://doi.org/10.1002/2014gl060457>, 2014.
- 674 Givnish, T. J.: Ecological aspects of plant morphology: leaf form in relation to environment, Acta  
675 Biotheoretica, 27, 83-142, 1978.
- 676 Givnish, T. J.: Adaptation to sun and shade: a whole-plant perspective, Australian Journal of Plant  
677 Physiology, 15, 63-92, <https://doi.org/10.1071/PP9880063>, 1988.
- 678 Glasspool, I. J. and Scott, A. C.: Phanerozoic concentrations of atmospheric oxygen reconstructed from  
679 sedimentary charcoal, Nature Geoscience, 3, 627-630, <https://doi.org/10.1038/ngeo923>, 2010.
- 680 Graham, H. V., Patzkowsky, M. E., Wing, S. L., Parker, G. G., Fogel, M. L., and Freeman, K. H.: Isotopic  
681 characteristics of canopies in simulated leaf assemblages, Geochimica et Cosmochimica Acta, 144, 82-95,  
682 <https://doi.org/10.1016/j.gca.2014.08.032>, 2014.
- 683 Grein, M., Utescher, T., Wilde, V., and Roth-Nebelsick, A.: Reconstruction of the middle Eocene climate  
684 of Messel using palaeobotanical data, Neues Jahrbuch Für Geologie und Paläontologie  
685 Abhandlungen, 260, 305-318, <https://doi.org/10.1127/0077-7749/2011/0139>, 2011a.
- 686 Grein, M., Konrad, W., Wilde, V., Utescher, T., and Roth-Nebelsick, A.: Reconstruction of atmospheric  
687 CO<sub>2</sub> during the early Middle Eocene by application of a gas exchange model to fossil plants from  
688 the Messel Formation, Germany, Palaeogeography Palaeoclimatology Palaeoecology, 309, 383-  
689 391, <https://doi.org/10.1016/j.palaeo.2011.07.008>, 2011b.
- 690 Grein, M., Oehm, C., Konrad, W., Utescher, T., Kunzmann, L., and Roth-Nebelsick, A.: Atmospheric CO<sub>2</sub>  
691 from the late Oligocene to early Miocene based on photosynthesis data and fossil leaf

- 692 characteristics, *Palaeogeography Palaeoclimatology Palaeoecology*, 374, 41-51,  
693 <https://doi.org/10.1016/j.palaeo.2012.12.025>, 2013.
- 694 Hashimoto, S., Tanaka, N., Suzuki, M., Inoue, A., Takizawa, H., Kosaka, I., Tanaka, K., Tantasirin, C., and  
695 Tangtham, N.: Soil respiration and soil CO<sub>2</sub> concentration in a tropical forest, Thailand, *Journal of  
696 Forest Research*, 9, 75-79, <https://doi.org/10.1007/s10310-003-0046-y>, 2004.
- 697 Haworth, M., Heath, J., and McElwain, J. C.: Differences in the response sensitivity of stomatal index to  
698 atmospheric CO<sub>2</sub> among four genera of Cupressaceae conifers, *Annals of Botany*, 105, 411-418,  
699 <https://doi.org/10.1093/aob/mcp309>, 2010.
- 700 Helliker, B. R. and Richter, S. L.: Subtropical to boreal convergence of tree-leaf temperatures, *Nature*,  
701 454, 511-514, <https://doi.org/10.1038/nature07031>, 2008.
- 702 Hirano, T., Kim, H., and Tanaka, Y.: Long-term half-hourly measurement of soil CO<sub>2</sub> concentration and  
703 soil respiration in a temperate deciduous forest, *Journal of Geophysical Research*, 108, 4631,  
704 <https://doi.org/10.1029/2003JD003766>, 2003.
- 705 Holtum, J. and Winter, K.: Are plants growing close to the floors of tropical forests exposed to markedly  
706 elevated concentrations of carbon dioxide?, *Australian Journal of Botany*, 49, 629-636,  
707 <https://doi.org/10.1071/BT00054>, 2001.
- 708 Jones, H. G.: *Plants and Microclimate*, Cambridge University Press, Cambridge, 1992.
- 709 Keeling, C. D.: The concentration and isotopic abundances of atmospheric carbon dioxide in rural areas,  
710 *Geochimica et Cosmochimica Acta*, 13, 322-334, [https://doi.org/10.1016/0016-7037\(58\)90033-4](https://doi.org/10.1016/0016-7037(58)90033-4), 1958.
- 712 Konrad, W., Roth-Nebelsick, A., and Grein, M.: Modelling of stomatal density response to atmospheric  
713 CO<sub>2</sub>, *Journal of Theoretical Biology*, 253, 638-658, <https://doi.org/10.1016/j.jtbi.2008.03.032>,  
714 2008.
- 715 Konrad, W., Katul, G., Roth-Nebelsick, A., and Grein, M.: A reduced order model to analytically infer  
716 atmospheric CO<sub>2</sub> concentration from stomatal and climate data, *Advances in Water Resources*,  
717 104, 145-157, <https://doi.org/10.1016/j.advwatres.2017.03.018>, 2017.
- 718 Kowalczyk, J. B., Royer, D. L., Miller, I. M., Anderson, C. W., Beerling, D. J., Franks, P. J., Grein, M.,  
719 Konrad, W., Roth-Nebelsick, A., Bowring, S. A., Johnson, K. R., and Ramezani, J.: Multiple proxy  
720 estimates of atmospheric CO<sub>2</sub> from an early Paleocene rainforest, *Paleoceanography and  
721 Paleoclimatology*, 33, 1427-1438, <https://doi.org/10.1029/2018PA003356>, 2018.
- 722 Kürschner, W. M.: The anatomical diversity of recent and fossil leaves of the durmast oak (*Quercus  
723 petraea* Lieblein/*Q. pseudocastanea* Goepert)-implications for their use as biosensors of  
724 palaeoatmospheric CO<sub>2</sub> levels, *Review of Palaeobotany and Palynology*, 96, 1-30,  
725 [https://doi.org/10.1016/S0034-6667\(96\)00051-6](https://doi.org/10.1016/S0034-6667(96)00051-6), 1997.
- 726 Kuznetsova, A., Brockhoff, P. B., and Christensen, R. H. B.: lmerTest package: tests in linear mixed effects  
727 models, *Journal of Statistical Software*, 82, <https://doi.org/10.18637/jss.v082.i13>, 2017.
- 728 Lei, X., Du, Z., Du, B., Zhang, M., and Sun, B.: Middle Cretaceous pCO<sub>2</sub> variation in Yumen, Gansu  
729 Province and its response to the climate events, *Acta Geologica Sinica*, 92, 801-813,  
730 <https://doi.org/doi:10.1111/1755-6724.13555>, 2018.
- 731 Lenton, T. M., Daines, S. J., and Mills, B. J. W.: COPSE reloaded: an improved model of biogeochemical  
732 cycling over Phanerozoic time, *Earth-Science Reviews*, 178, 1-28,  
733 <https://doi.org/10.1016/j.earscirev.2017.12.004>, 2018.
- 734 Lloyd, J., Kruijt, B., Hollinger, D. Y., Grace, J., Francey, R. J., Wong, S.-C., Kelliher, F. M., Miranda, A. C.,  
735 Farquhar, G. D., and Gash, J.: Vegetation effects on the isotopic composition of atmospheric CO<sub>2</sub>  
736 at local and regional scales: theoretical aspects and a comparison between rain forest in  
737 Amazonia and a boreal forest in Siberia, *Australian Journal of Plant Physiology*, 23, 371-399,  
738 <https://doi.org/10.1071/PP9960371>, 1996.

- 739 Londoño, L., Royer, D. L., Jaramillo, C., Escobar, J., Foster, D. A., Cárdenas-Rozo, A. L., and Wood, A.:  
740 Early Miocene CO<sub>2</sub> estimates from a Neotropical fossil assemblage exceed 400 ppm, American  
741 Journal of Botany, 105, 1929-1937, <https://doi.org/10.1002/ajb2.1187>, 2018.
- 742 Marrero, T. R. and Mason, E. A.: Gaseous diffusion coefficients, Journal of Physical and Chemical  
743 Reference Data, 1, 3-118, <https://doi.org/10.1063/1.3253094>, 1972.
- 744 Maxbauer, D. P., Royer, D. L., and LePage, B. A.: High Arctic forests during the middle Eocene supported  
745 by moderate levels of atmospheric CO<sub>2</sub>, Geology, 42, 1027-1030,  
746 <https://doi.org/10.1130/g36014.1>, 2014.
- 747 McElwain, J. C.: Do fossil plants signal palaeoatmospheric CO<sub>2</sub> concentration in the geological past?,  
748 Philosophical Transactions of the Royal Society London B, 353, 83-96,  
749 <https://doi.org/10.1098/rstb.1998.0193>, 1998.
- 750 McElwain, J. C. and Chaloner, W. G.: Stomatal density and index of fossil plants track atmospheric  
751 carbon dioxide in the Palaeozoic, Annals of Botany, 76, 389-395,  
752 <https://doi.org/10.1006/anbo.1995.1112>, 1995.
- 753 McElwain, J. C. and Chaloner, W. G.: The fossil cuticle as a skeletal record of environmental change,  
754 Palaios, 11, 376-388, <https://doi.org/10.2307/3515247>, 1996.
- 755 McElwain, J. C., Montañez, I., White, J. D., Wilson, J. P., and Yiotis, C.: Was atmospheric CO<sub>2</sub> capped at  
756 1000 ppm over the past 300 million years?, Palaeogeography Palaeoclimatology Palaeoecology,  
757 441, 653-658, <https://doi.org/http://dx.doi.org/10.1016/j.palaeo.2015.10.017>, 2016.
- 758 Medina, E., Montes, G., Cuevas, E., and Rokzandic, Z.: Profiles of CO<sub>2</sub> concentration and δ<sup>13</sup>C values in  
759 tropical rain forests of the upper Rio Negro Basin, Venezuela, Journal of Tropical Ecology, 2, 207-  
760 217, <https://doi.org/10.1017/S0266467400000821>, 1986.
- 761 Michaletz, S. T., Weiser, M. D., Zhou, J., Kaspari, M., Helliker, B. R., and Enquist, B. J.: Plant  
762 thermoregulation: energetics, trait-environment interactions, and carbon economics, Trends in  
763 Ecology & Evolution, 30, 714-724, <https://doi.org/10.1016/j.tree.2015.09.006>, 2015.
- 764 Michaletz, S. T., Weiser, M. D., McDowell, N. G., Zhou, J., Kaspari, M., Helliker, B. R., and Enquist, B. J.:  
765 The energetic and carbon economic origins of leaf thermoregulation, Nature Plants, 2, 16129,  
766 <https://doi.org/10.1038/nplants.2016.129>, 2016.
- 767 Milligan, J. N., Royer, D. L., Franks, P. J., Upchurch, G. R., and McKee, M. L.: No evidence for a large  
768 atmospheric CO<sub>2</sub> spike across the Cretaceous-Paleogene boundary, Geophysical Research  
769 Letters, 46, xxx-xxx, <https://doi.org/10.1029/2018GL081215>, 2019.
- 770 Mills, B. J. W., Belcher, C. M., Lenton, T. M., and Newton, R. J.: A modeling case for high atmospheric  
771 oxygen concentrations during the Mesozoic and Cenozoic, Geology, 44, 1023-1026,  
772 <https://doi.org/10.1130/g38231.1>, 2016.
- 773 Montañez, I. P., McElwain, J. C., Poulsen, C. J., White, J. D., DiMichele, W. A., Wilson, J. P., Griggs, G., and  
774 Hren, M. T.: Climate, p<sub>CO<sub>2</sub></sub> and terrestrial carbon cycle linkages during late Palaeozoic glacial-  
775 interglacial cycles, Nature Geoscience, 9, 824-828, <https://doi.org/10.1038/ngeo2822>, 2016.
- 776 Munger, W. and Hadley, J.: CO<sub>2</sub> profile at Harvard Forest HEM and LPH towers since 2009, Harvard  
777 Forest Data Archive: HF197,  
778 <http://harvardforest.fas.harvard.edu:8080/exist/apps/datasets/showData.html?id=hf197>, 2017.
- 779 NOAA/ESRL: <https://www.esrl.noaa.gov/gmd/ccgg/trends/data.html>, 2019.
- 780 Porter, A. S., Yiotis, C., Montañez, I. P., and McElwain, J. C.: Evolutionary differences in Δ<sup>13</sup>C detected  
781 between spore and seed bearing plants following exposure to a range of atmospheric O<sub>2</sub>:CO<sub>2</sub>  
782 ratios: implications for paleoatmosphere reconstruction, Geochimica et Cosmochimica Acta,  
783 213, 517-533, <https://doi.org/10.1016/j.gca.2017.07.007>, 2017.
- 784 Quay, P., King, S., Wilbur, D., Wofsy, S., and Rickey, J.: <sup>13</sup>C/<sup>12</sup>C of atmospheric CO<sub>2</sub> in the Amazon Basin:  
785 forest and river sources, Journal of Geophysical Research, 94, 18327-18336,  
786 <https://doi.org/10.1029/JD094iD15p18327>, 1989.

- 787 R Core Team: R: A Language and Environment for Statistical Computing, R Foundation for Statistical  
788 Computing, Vienna, Austria, <https://www.R-project.org/>, 2016.
- 789 Reichgelt, T., D'Andrea, W. J., and Fox, B. R. S.: Abrupt plant physiological changes in southern New  
790 Zealand at the termination of the Mi-1 event reflect shifts in hydroclimate and  $p\text{CO}_2$ , Earth and  
791 Planetary Science Letters, 455, 115-124, <https://doi.org/10.1016/j.epsl.2016.09.026>, 2016.
- 792 Richey, J. D., Upchurch, G. R., Montañez, I. P., Lomax, B. H., Suarez, M. B., Crout, N. M. J., Joeckel, R. M.,  
793 Ludvigson, G. A., and Smith, J. J.: Changes in  $\text{CO}_2$  during Ocean Anoxic Event 1d indicate  
794 similarities to other carbon cycle perturbations, Earth and Planetary Science Letters, 491, 172-  
795 182, <https://doi.org/10.1016/j.epsl.2018.03.035>, 2018.
- 796 Roeske, C. and O'Leary, M. H.: Carbon isotope effects on enzyme-catalyzed carboxylation of ribulose  
797 bisphosphate, Biochemistry, 23, 6275-6284, <https://doi.org/10.1021/bi00320a058>, 1984.
- 798 Roth-Nebelsick, A., Grein, M., Utescher, T., and Konrad, W.: Stomatal pore length change in leaves of  
799 *Eotrigonobalanus furcinervis* (Fagaceae) from the Late Eocene to the Latest Oligocene and its  
800 impact on gas exchange and  $\text{CO}_2$  reconstruction, Review of Palaeobotany and Palynology, 174,  
801 106-112, <https://doi.org/10.1016/j.revpalbo.2012.01.001>, 2012.
- 802 Roth-Nebelsick, A., Oehm, C., Grein, M., Utescher, T., Kunzmann, L., Friedrich, J.-P., and Konrad, W.:  
803 Stomatal density and index data of *Platanus neptuni* leaf fossils and their evaluation as a  $\text{CO}_2$   
804 proxy for the Oligocene, Review of Palaeobotany and Palynology, 206, 1-9,  
805 <https://doi.org/10.1016/j.revpalbo.2014.03.001>, 2014.
- 806 Roth, J. and Dilcher, D.: Some considerations in leaf size and leaf margin analysis of fossil leaves, Courier  
807 Forschungsinstitut Senckenberg, 30, 165-171, 1978.
- 808 Royer, D. L.: Stomatal density and stomatal index as indicators of paleoatmospheric  $\text{CO}_2$  concentration,  
809 Review of Palaeobotany and Palynology, 114, 1-28, [https://doi.org/10.1016/S0034-6667\(00\)00074-9](https://doi.org/10.1016/S0034-6667(00)00074-9), 2001.
- 810 Royer, D. L. and Hren, M. T.: Carbon isotopic fractionation between whole leaves and cuticle, Palaios, 32,  
811 199-205, <https://doi.org/10.2110/palo.2016.073>, 2017.
- 812 Royer, D. L., Miller, I. M., Peppe, D. J., and Hickey, L. J.: Leaf economic traits from fossils support a weedy  
813 habit for early angiosperms, American Journal of Botany, 97, 438-445,  
814 <https://doi.org/10.3732/ajb.0900290>, 2010.
- 815 Sack, L. and Scoffoni, C.: Leaf venation: structure, function, development, evolution, ecology and  
816 applications in the past, present and future, New Phytologist, 198, 983-1000,  
817 <https://doi.org/10.1111/nph.12253>, 2013.
- 818 Sack, L., Melcher, P. J., Liu, W. H., Middleton, E., and Pardee, T.: How strong is intracanopy leaf plasticity  
819 in temperate deciduous trees?, American Journal of Botany, 93, 829-839,  
820 <https://doi.org/10.3732/ajb.93.6.829>, 2006.
- 821 Schubert, B. A. and Jahren, A. H.: Incorporating the effects of photorespiration into terrestrial  
822 paleoclimate reconstruction, Earth-Science Reviews, 177, 637-642,  
823 <https://doi.org/10.1016/j.earscirev.2017.12.008>, 2018.
- 824 Smith, R. Y., Greenwood, D. R., and Basinger, J. F.: Estimating paleoatmospheric  $p\text{CO}_2$  during the Early  
825 Eocene Climatic Optimum from stomatal frequency of *Ginkgo*, Okanagan Highlands, British  
826 Columbia, Canada, Palaeogeography Palaeoclimatology Palaeoecology, 293, 120-131,  
827 <https://doi.org/10.1016/j.palaeo.2010.05.006>, 2010.
- 828 Song, X., Barbour, M. M., Saurer, M., and Helliker, B. R.: Examining the large-scale convergence of  
829 photosynthesis-weighted tree leaf temperatures through stable oxygen isotope analysis of  
830 multiple data sets, New Phytologist, 192, 912-924, <https://doi.org/10.1111/j.1469-8137.2011.03851.x>, 2011.

- 833 Sotta, E. D., Meir, P., Malhi, Y., Donato nobre, A., Hodnett, M., and Grace, J.: Soil CO<sub>2</sub> efflux in a tropical  
834 forest in the central Amazon, *Global Change Biology*, 10, 601-617,  
835 <https://doi.org/10.1111/j.1529-8817.2003.00761.x>, 2004.
- 836 Spicer, R. A.: The importance of depositional sorting to the biostratigraphy of plant megafossils, in:  
837 *Biostratigraphy of Fossil Plants: Successional and Paleoecological Analyses*, edited by: Dilcher, D.  
838 and Taylor, T., Dowden, Hutchinson, and Ross, Stroudsburg, PA, 171-183, 1980.
- 839 Sternberg, L., Mulkey, S. S., and Wright, S. J.: Ecological interpretation of leaf carbon isotope ratios:  
840 influence of respired carbon dioxide, *Ecology*, 70, 1317-1324, <https://doi.org/10.2307/1938191>,  
841 1989.
- 842 Stevens, P. F.: Angiosperm Phylogeny Website. Version 13., [www.mobot.org/MOBOT/research/APweb/](http://www.mobot.org/MOBOT/research/APweb/),  
843 2001 onwards.
- 844 Talbert, C. M. and Holch, A. E.: A study of the lobing of sun and shade leaves, *Ecology*, 38, 655-658,  
845 <https://doi.org/10.2307/1943135>, 1957.
- 846 Tcherkez, G.: How large is the carbon isotope fractionation of the photorespiratory enzyme glycine  
847 decarboxylase?, *Functional Plant Biology*, 33, 911-920, <https://doi.org/10.1071/FP06098>, 2006.
- 848 Tesfamichael, T., Jacobs, B., Tabor, N., Michel, L., Currano, E., Feseha, M., Barclay, R., Kappelman, J., and  
849 Schmitz, M.: Settling the issue of “decoupling” between atmospheric carbon dioxide and global  
850 temperature: [CO<sub>2</sub>]<sub>atm</sub> reconstructions across the warming Paleogene-Neogene divide, *Geology*,  
851 45, 999-1002, <https://doi.org/10.1130/G39048.1>, 2017.
- 852 Tipple, B. J., Meyers, S. R., and Pagani, M.: Carbon isotope ratio of Cenozoic CO<sub>2</sub>: a comparative  
853 evaluation of available geochemical proxies, *Paleoceanography*, 25, PA3202,  
854 <https://doi.org/10.1029/2009PA001851>, 2010.
- 855 Uhl, D. and Mosbrugger, V.: Leaf venation density as a climate and environmental proxy: a critical review  
856 and new data, *Palaeogeography Palaeoclimatology Palaeoecology*, 149, 15-26,  
857 [https://doi.org/10.1016/S0031-0182\(98\)00189-8](https://doi.org/10.1016/S0031-0182(98)00189-8), 1999.
- 858 Von Caemmerer, S.: Biochemical Models of Leaf Photosynthesis, CSIRO Publishing, Collingwood,  
859 Australia, 2000.
- 860 Wang, Y., Ito, A., Huang, Y., Fukushima, T., Wakamatsu, N., and Momohara, A.: Reconstruction of  
861 altitudinal transportation range of leaves based on stomatal evidence: an example of the Early  
862 Pleistocene *Fagus* leaf fossils from central Japan, *Palaeogeography, Palaeoclimatology,*  
863 *Palaeoecology*, 505, 317-325, <https://doi.org/10.1016/j.palaeo.2018.06.011>, 2018.
- 864 Woodward, F. I.: Stomatal numbers are sensitive to increases in CO<sub>2</sub> from pre-industrial levels, *Nature*,  
865 327, 617-618, <https://doi.org/10.1038/327617a0>, 1987.
- 866 Woodward, F. I. and Kelly, C. K.: The influence of CO<sub>2</sub> concentration on stomatal density, *New*  
867 *Phytologist*, 131, 311-327, <https://doi.org/10.1111/j.1469-8137.1995.tb03067.x>, 1995.
- 868 Wynn, J. G.: Towards a physically based model of CO<sub>2</sub>-induced stomatal frequency response, *New*  
869 *Phytologist*, 157, 391-398, <https://doi.org/10.1046/j.1469-8137.2003.00702.x>, 2003.